crystals

MDPI

*Review*

# Layered Double Hydroxides in Bioinspired Nanotechnology

**Giuseppe Arrabito [1,*], Riccardo Pezzilli [2], Giuseppe Prestopino [2,*] and Pier Gianni Medaglia [2]**

[1] Dipartimento di Fisica e Chimica—Emilio Segrè, Università di Palermo, Viale delle Scienze, Edificio 17, 90128 Palermo, Italy

[2] Dipartimento di Ingegneria Industriale, Università di Roma "Tor Vergata", Via del Politecnico 1, 00133 Roma, Italy; riccardo.pezzilli@gmail.com (R.P.); medaglia@uniroma2.it (P.G.M.)

* Correspondence: giuseppedomenico.arrabito@unipa.it (G.A.); giuseppe.prestopino@uniroma2.it (G.P.)

Received: 26 May 2020; Accepted: 6 July 2020; Published: 11 July 2020


**Abstract:** Layered Double Hydroxides (LDHs) are a relevant class of inorganic lamellar nanomaterials that have attracted significant interest in life science-related applications, due to their highly controllable synthesis and high biocompatibility. Under a general point of view, this class of materials might have played an important role for the origin of life on planet Earth, given their ability to adsorb and concentrate life-relevant molecules in sea environments. It has been speculated that the organic–mineral interactions could have permitted to organize the adsorbed molecules, leading to an increase in their local concentration and finally to the emergence of life. Inspired by nature, material scientists, engineers and chemists have started to leverage the ability of LDHs to absorb and concentrate molecules and biomolecules within life-like compartments, allowing to realize highly-efficient bioinspired platforms, usable for bioanalysis, therapeutics, sensors and bioremediation. This review aims at summarizing the latest evolution of LDHs in this research field under an unprecedented perspective, finally providing possible challenges and directions for future research.

**Keywords:** origin of life; DNA; layer double hydroxide; synthetic biology; bioinspired devices; biosensors; bioanalysis

## 1. Introduction

Layered double hydroxides (LDHs) are an important class of two-dimensional (2D) layered materials belonging to the group of hydrotalcite-like (HT) compounds [1–4]. They are constituted by stacks of positively charged hydroxyl layers of bivalent ions (e.g., $Ca^{2+}$, $Zn^{2+}$, $Mg^{2+}$ and $Ni^{2+}$) and trivalent metallic ions (e.g., $Al^{3+}$, $Fe^{3+}$, $Cr^{3+}$ and $In^{3+}$). The isomorphic substitution of some of the bivalent metal ions by the trivalent metal ions forms a positive residual charge on the metal-hydroxide framework, which is in turn balanced by exchangeable interlayer anions to maintain the global electroneutrality. The general formula of LDHs is $[M_{1-x}{}^{2+}M_x{}^{3+}(OH)_2]^{x+}\cdot[A_{x/n}]^{n-}\cdot mH_2O$, where $M^{2+}$ and $M^{3+}$ are the divalent and trivalent metal ions, respectively; $A^{n-}$ are inorganic or organic anions; $m$ is the number of interlayer water; and $x = M^{3+}/(M^{2+} + M^{3+})$ is the layer charge density, or molar ratio [5]. It is worth pointing out that, in LDHs, the electric charge of the layers and of the interlayer ions is the opposite of that found in the vast majority of layered materials such as silicate clays (cationic clays), which feature negatively charged host layers and exchangeable cations in the interlayer spaces. Indeed, LDHs are also usually known as anionic clays [6]. Their unique physicochemical properties [7], i.e., biocompatibility, lamellar structure and compositional diversity, make them suitable for adsorption processes of a large variety of molecules, ranging from organic molecules to biomacromolecules.

LDHs also play a prominent role in photocatalysis [8] and, more recently, in many life sciences related applications [9], especially for biosensors [10], drug delivery [11] and tissue bioengineering [12]. In the last years, the application of LDHs and their composites in biological, chemical and environmental processes have been extensively reviewed [13–16].

In particular, the role of LDHs as catalysts in relevant organic chemistry reactions, as photocatalytic centers, and their emerging application in cellular biology were extensively summarized in a previous review from our group [5]. Notably, the well-investigated chemistry- and biology-related applications of LDHs summarized in that review article highlight the conspicuous studies focused on the synthesis, characterization and applications of LDH-based systems. In fact, similar to ZnO-materials [17,18], LDHs can be synthesized under mild conditions [19] following the coprecipitation method, which consists in the addition of a basic substance to an aqueous solution containing the salts of two different metals, namely $M^{2+}$ and $M^{3+}$, leading to the precipitation of the metal hydroxides, with the subsequent formation of LDHs [20–22]. Such synthetic approach can be leveraged to produce LDH materials on demand, with the desired chemical composition, aggregation state and particle size [15]. The latter can be tuned ranging from nanoclusters [23] to micron scale [24]. Notably, highly porous and highly dispersed LDHs with high surface area allow the full potential of LDH-based compounds to be efficiently exploited in many applications, such as heterogeneous catalysis and catalyst supports. Single layer LDHs are also ideal building blocks for functional assembly. However, the LDHs synthesized by conventional coprecipitation methods tend to easily aggregate, due to electrostatic interactions, interlamellar hydrogen bonding networks and their hydrophilic nature [25], thus resulting in low surface area and large particle size. To overcome these issues, many research efforts have optimized down to single- or few-layer nanosheets. Delamination of LDHs into single layers in polar solvents, such as formamide, butanol and acrylate, is a well-known process, as extensively reviewed by Wang and O'Hare [26]. In this context, it is worth mentioning that carbonate ($CO_3^{2-}$) contamination during both synthesis and post-treatment processes complicates LDH delamination, to such an extent that the direct exfoliation of a $CO_3^{2-}$-LDH is believed to be almost impossible [27]. The conventional approach to overcome this consists in the development of anion-exchange protocols to replace carbonate ions with other intercalating anions featuring weaker electrostatic interactions with the LDH structure [25,28]. Recently, a direct exfoliation method of $CO_3^{2-}$-LDHs, which avoids anion-exchange reactions, using liquid phase delamination via ultrasonic tip has been demonstrated [29]. Ecofriendly delamination approaches constituted by washing/stirring the LDH dispersion in decarbonated water have also been reported [30–32]. Isolation and recovery of delaminated LDHs without aggregation is a big challenge hindering practical application and commercial exploitation. In the last years, with the aim to increase LDH dispersion and organophilicity and to fabricate stable delaminated LDH dry powders, O'Hare and coworkers developed post-treatment routes for LDHs using both aqueous miscible organic (AMO-LDHs) and aqueous immiscible (AIM-LDHs) organic solvents, yielding highly porous, highly dispersed LDH powders of exfoliated nanosheets [33,34]. Some experimental protocols also permit films of interconnected LDH nanoplatelets to be grown onto aluminum surfaces as hierarchically nanostructured coatings by soaking aluminum thick foils in an aqueous solution containing a soluble zinc salt [35–39]. In this case, the trivalent ions ($Al^{3+}$) are provided by the sacrificial aluminum foil, whose role is both reactant and substrate, and ultimately allows the LDH film adhesion to be improved. LDH-based materials have triggered conspicuous studies in the field of organic chemistry, mainly due to their excellent ability as heterogeneous catalysts for the preparation of fine chemicals, intermediates and valuable molecules, benefiting from the simplicity of their preparation from cheap and non-harmful precursors, and the low toxicity of their possibly produced decomposition products [5]. The high reactivity of LDHs is related to their layered structure which features a high anion-exchange capability [40–44], and to their high basicity, due to either structural hydroxyl anions in hydrated material or $O^{2-}$-$M^{n+}$ pairs in the case of water-free calcined material [45]. A crucial feature is also represented by the metal ratio. In fact, the incorporation of specific metals in the octahedral layer can produce LDH compounds with unexpected and novel properties, as well as modulate the existing

chemical reactivity. It is worth mentioning literature where the arrangement of cations within the LDH lattice is discussed. As a matter of fact, the ordering of cations is believed to have crucial effects on many of the physicochemical properties of LDHs, affecting the charge density of the metal hydroxide sheets, and the overall bonding, mobility, orientation and reactivity of the chemical species in the interlayer space and on the surface [46–49]. In particular, the $M^{2+}$-$M^{3+}$ cation order is important for the catalytic activity of LDHs [50], and the different distribution of the $M^{3+}$ cation in the $M^{2+}$ matrix regulates interlayer anionic charge and, in turn, intercalation reactions [51].

The intriguing catalytic properties and the high compatibility with biological systems of LDHs continuously open new research directions. Among them, up-to-date research topics of interest both for fundamental research and applications come from the presumed role of LDHs in the evolution of natural systems and, in turn, from the realization of a novel class of LDH-based life-inspired devices. As a matter of fact, the path permitting a complete understanding of the role of LDHs within the origin of life is still unclear and needs more research. However, some studies point out their possible role in this exciting research field. In fact, cationic clays and LDHs [52,53] might have played an important role for the origin of life on planet Earth, having triggered the formation of life-relevant prebiotic settings through the evolution of molecular systems, leading to the formation of polymerized molecules and finally to the emergence of life [54]. In a pre-biological Earth model, the ion exchange properties arising from the positively charged sites in LDHs allowed the latter to concentrate amino acids, and to safely promote biopolymer formation, offering also protection from the effects of UV irradiation. A mechanism of prebiotic information storage and transfer in LDH matrices based on replication and conservation of $M^{2+}$-$M^{3+}$ cation arrangements was also proposed by Greenwell and Coveney [55]. In a sort of reverse evolutionary process, in the recent years, learning from nature, researchers have conceived the concepts of biomimetism and bioinspiration [56] in nanomaterials science to achieve unprecedented advanced functionalities based on designs that referred to structures in living creatures [57–61]. Under this exciting perspective, the most recent studies in the field of LDHs are striving to recapitulate life-like scenarios in the construction of hybrid LDH-based platforms, mimicking compositions or structures of natural species (e.g., biological macromolecules and microorganisms), with the aim to further improve their efficiency and their sustainability in the context of the natural environment [62,63]. Indeed, the low cost, biocompatibility and extraordinary adaptability of LDHs in many different purposes have allowed the effective application of bioinspired synthesis routes to LDH-based assembly of nanostructured materials and devices, which combine the eco-friendly nature of these materials and their versatility in the context of materials science. Another intriguing strategy to achieve bio-functionalization consists in associating biological species (e.g., amino acids, nucleosides, oligo nucleotides, DNA, proteins and enzymes) to LDH host matrices, as recently reviewed by Forano et al. [15] for LDH-biohybrids based on immobilization of bacteria and algae.

Motivated by the emerging role of bioinspired nanomaterials research, we felt the need to review the role of LDHs in this scenario, by investigating the fundamental science aspects and the possible emerging nanotechnology-related applications. At first, the present review provides an insight into the link between the role of LDHs in the origin of life, in particular focusing on their catalytic activities that promoted the formation of pre-biotic molecules and the possibility to fabricate artificial LDHs-based artificial compartments to mimic prebiotic platforms. These studies are speculative, mostly driven by the willingness to explore basic aspects of LDHs in their possible but still not completely clear role within the topic of origin of life. Secondly, this review updates and extends our previously review article [5], covering different aspects and, more in general, aiming at bridging fundamental science with new approaches that may support the design of LDH-based systems for the fabrication of life-like and life-inspired devices, especially in the fields of composites and coatings, sensors, life-inspired catalysis and bioremediation. To guide the reader, this review is divided into the following sections: the role of clays in the origin of life (Section 2), LDH interaction with biomolecules (Section 3), LDH-based compartments fabrication (Section 4), LDH-bioinspired devices assembly (Section 5) and finally the conclusions and perspectives (Section 6).

## 2. The Role of Clays in the Origin of Life

The origin of life (or abiogenesis) is among the most intriguing questions in science [64]. Although it is not possible to know all the details of this process, some scientific hypotheses attempt to explain the synthesis of the molecules which were necessary for the emergence of primitive forms of life in planet Earth 3.8 billion years ago [65] as deriving from a reducing atmosphere (Miller's experiment [66]), meteorites impacts [67] or from metal sulfides in deep-sea hydrothermal vents, as explained in the famous article of Russel [68]. Recent studies from Das at al. [69] leveraged computational methods to shed light on the role of hydrogen cyanide (HCN) as a source of ribonucleic acid (RNA) and protein precursors. The authors also argued that just the interaction of HCN with water would have sufficed to trigger a series of reactions leading to the life-essential precursors (nucleic acids and proteins), as reported in Figure 1.

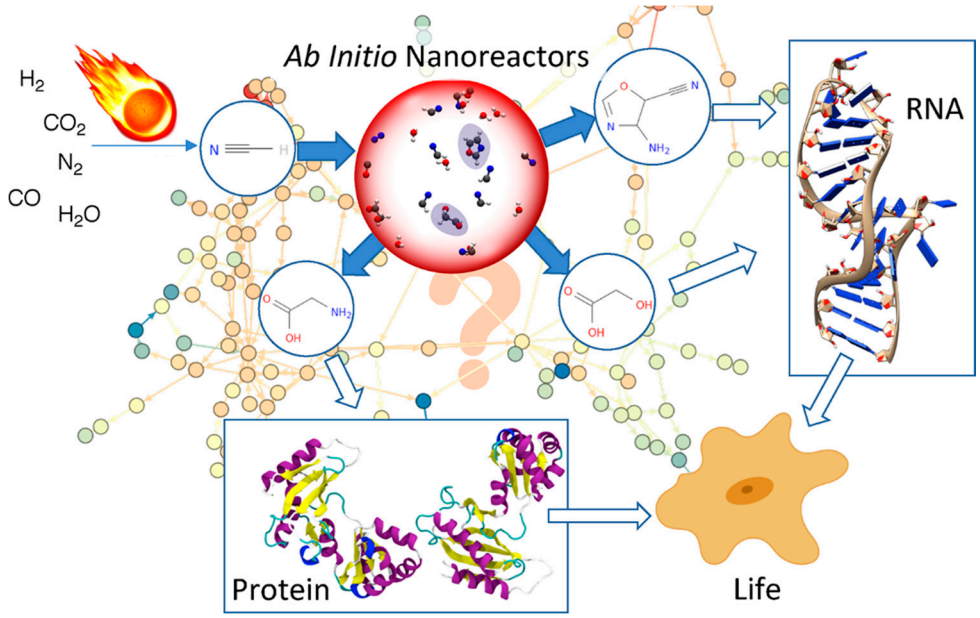


**Figure 1.** The synthesis of life relevant molecules (RNA, proteins) starting from inorganic materials and leading to the onset of chemical evolution. Figure reproduced from Ref. [70] https://pubs.acs.org/doi/10.1021/acscentsci.9b00832; Copyright (2019) American Chemical Society, further permissions related to the material excerpted should be directed to the ACS.

Once prebiotic molecules formed in water, cationic and anionic clays were also present on the surface of the Earth and could then interact with prebiotic molecules. In fact, whereas the probability that molecules could encounter in a 3D liquid environment is quite low, the solid mineral surfaces permitted to adsorbed molecules and permit them to interact and react [71]. According to some theories, radionuclide-induced defect sites in iron-rich minerals could have triggered the formation of prebiotic life [72]. Among all the possible hypothesis for the origin of life, one of the most relevant is that of hydrothermal vents [73], since they provided the possible evolutionary transition from geochemical to biochemical processes in absence of sun light. Hydrothermal vents are crevices in the seafloor from which geothermally heated water pours into ocean water. Among them, alkaline vents (such as the Lost City hydrothermal field) could have acted as ideal electrochemical flow reactors in the ocean during the Hadean period [74], in which the ocean waters were acidic since they were rich in $CO_2$. More specifically, within these hydrothermal vents, a pH gradient was formed between inorganic micropores barriers containing catalytic Fe(Ni)S minerals and the acidic ocean water, resulting in proton gradients similar to the proton-motive force required for carbon fixation in bacteria and archaea. The alkaline hydrothermal field provided serpentinization reactions that produced methane and hydrogen. Such pH energy

input, in addition to the catalysis provided by the Fe(Ni)S minerals, triggered the reduction of $CO_2$ with $H_2$ and the relative production of life-essential organic molecules, such as hydrocarbons, finally leading to the first primitive cellular systems. Within this scenario, the question that can arise is then if LDHs were present in the hydrothermal vents. To this regard, Cairns-Smith and Braterman speculated that inorganic $Fe^{2+}/Fe^{3+}$ LDHs (also defined green rust) [75] were at the sites of Archean oceanic hydrothermal vents, constituting one of the most-common components of early ocean sediments. The presence of this peculiar LDH can be ascribed to the lack of oxygen in the Archean atmosphere, permitting the presence of $Fe^{2+}$ in aqueous environments and oxidation and precipitation as $Fe^{III}OOH$. As explained by Russell [76], the green rust might have played a fundamental role in the formation of prebiotic life. In particular, within the alkaline vent model, the green rust precipitated forming individual compartments that permitted the formation of ionic gradients and catalytic centers for endergonic reactions, aided by sulfides and trace elements acting as catalytic promoters that led to the formation of pre-biotic molecules.

In this context, as first speculated by Bernal [77], clays likely played an important role in promoting the molecular organization and the formation of polymerized biomolecules (nucleotides and amino acids), given their potentially large adsorption capacity, the ability to shield molecules against ultraviolet radiation, concentrate organic chemicals and catalyze chemical polymerization reactions. Following the seminal proposal by Cairns-Smith [78], who postulated a concept of "genetic takeover", according to which carbon-based life may have gradually evolved from organic–inorganic complexes of clays with organic molecules, some remarkable experiments demonstrated that clay minerals played an active role in the abiotic origin of life. For instance, as elegantly demonstrated by Ferris [79], montmorillonite clays could have a role in the polymerization of short RNA oligomers (up to 50 mer). Similarly, the fluctuation of temperature and humidity could have triggered the amino acids polymerization in the presence of clay minerals [80]. Finally, clays could have increased the rate of formation of vesicles from fatty acid micelles, along with the possibility to encapsulate clay particles inside the vesicles in addition to RNA molecules adsorbed on the clay surfaces, as demonstrated by Szostak et al. using montmorillonite clay [81]. Once formed, such vesicles could grow by incorporating fatty acids and divide, thus mediating vesicle replication through cycles of growth and division. In this scenario, since the first hypotheses by Kuma et al. [52] and Arrhenius [53], there are not so many studies in this field that regard the role of LDHs, even if they are positively charged clays that can interact with negatively charged molecules. LDHs might have played a role in selecting DNA over RNA for genetic information, due to its ability in enhancing the Watson–Crick hydrogen-bonding when intercalated within the LDH interlayers, in comparison to RNA [55,82]. Grégoire et al. [83] also explored the possible role of LDHs in early Earth chemistry, leading to the formation of peptides. Very recently, Vasti et al. demonstrated that LDHs strongly interact with model lipid membranes [84]; these experiments could also highlight the role of LDHs in partitioning within the membranes of primitive cellular-like compartments. In a very recent hypothesis paper, Bernhardt [85] proposed that LDH clays might have promoted the synthesis of prebiotic precursors and also played other roles in the origin of life, such as in the formation of the first lipid bilayers.

The fundamental reaction that triggered aerobic life was the photosynthetic oxygen evolution, in which two water molecules produce four electrons and four protons used for the photosynthetic processes and molecular oxygen [86]. This reaction is catalyzed by a manganese-containing cofactor contained in photosystem II known as the oxygen-evolving complex. Mimicking natural systems, studies have demonstrated that LDHs can constitute ideal low-cost catalytic materials for the oxygen evolution [87], in which both the $M^{2+}$ and $M^{3+}$ take part to the redox reactions, as reported in Figure 2. Some relevant applications of LDHs as catalysts for oxygen evolution reaction (OER) are discussed in Section 5.3.

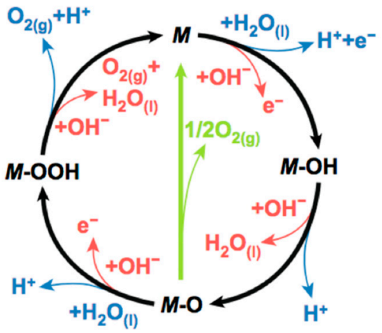


**Figure 2.** Simplified scheme for the oxygen evolution mechanism involving the formation of a peroxide (M–OOH) intermediate under acid (blue line) and alkaline (red line) reaction conditions. Reproduced from Ref. [87] under a Creative Commons Attribution 4.0 International License.

## 3. LDH Interaction with Biomolecules and Relevant Applications

### *3.1. Nucleic Acids*

Nucleotides are the key molecules for the storage and transmission of genetic information [88]. The chemistry of their synthesis and polymerization is still a matter of debate [89]; however, based on the observation from Bernal [77], they could have had a role in concentrating and even acting as catalyst to form oligonucleotides. Moreover, they could have also been involved in protecting nucleotide against decomposition in presence of ionizing radiation [90]. Nucleic acids are composed of nitrogenous organic bases, pentose and phosphoric acids, are a typical polyanion within hydrogen-bonding groups, and can therefore enter inside the LDH interlayer, forming a nucleic acid/inorganic composite stabilized by electrostatic interactions. Inspired by the ability to protect and store nucleotides and oligomers, DNA-LDH hybrids have found remarkable applications in the field of gene delivery to cells. The reason for this was investigated by Li et al. [91], who employed dissipative particle dynamic simulations for elucidating the interaction with cellular membranes at different levels (i.e., total or partial penetration vs. anchorage—see Figure 3), as a function of the lateral size and layer number. These results shed light on the very important role of layer thickness—i.e., the lower is the thickness, the higher the probability that DNA-LDHs hybrids can be internalized, and hence serve as gene delivery tool.

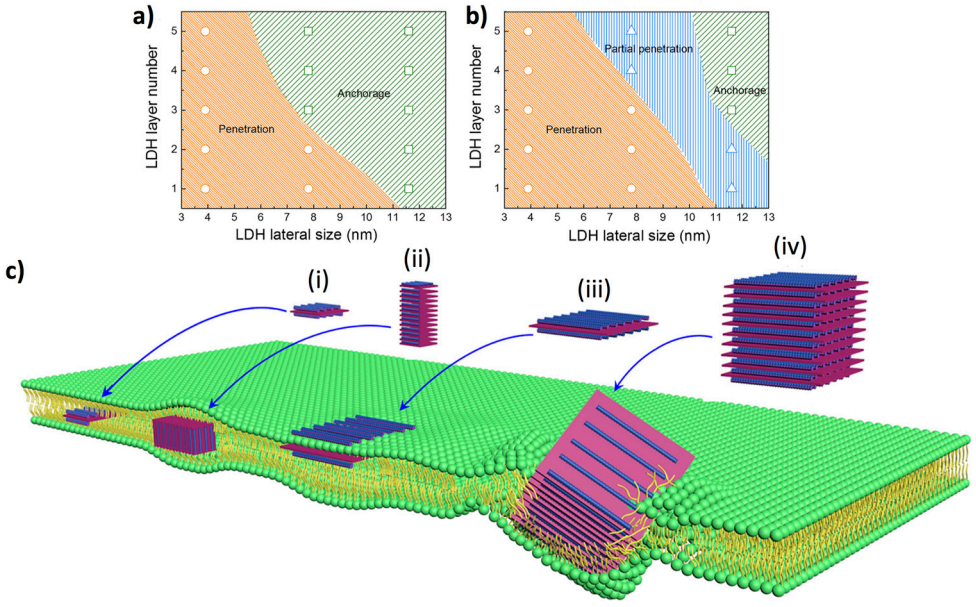


**Figure 3.** Interaction of DNA-LDH hybrids of different lateral layer sizes and thicknesses with model

cellular membranes. Relation between the LDH lateral size and LDH layer number at two different time points: 6.4 μs (**a**); and 32 μs (**b**). (**c**) Effect of the size of the DNA-LDH hybrids on the internalization. Reproduced from Ref. [91]. Copyright (2020), with permission from Elsevier.

### 3.2. Phospholipids

Cationic clays can effectively interact with living cells producing hybrid half inorganic viable structures, as demonstrated by Murase and Gonda [92] and Konnova et al. [93] in previous seminal studies on montmorillonite and hallosite clay nanotubes, respectively. Indeed, it was clarified that such clays can interact with phospholipids via electrostatic interactions [92], giving rise to apparently ordered phospholipids self-assembled layers, which can lead to *"armored cells"* if exposed to living cell membranes [93]. Notably, in the case of LDHs, the structural analysis from Itoh et al. [94] interestingly demonstrated, by means of spectroscopic and crystallographic characterizations, that stearate ions can form ordered bilayer structures within MgAl-LDH layers with a tilting angle of approximately 29° from the right angle of the layers (Figure 4).

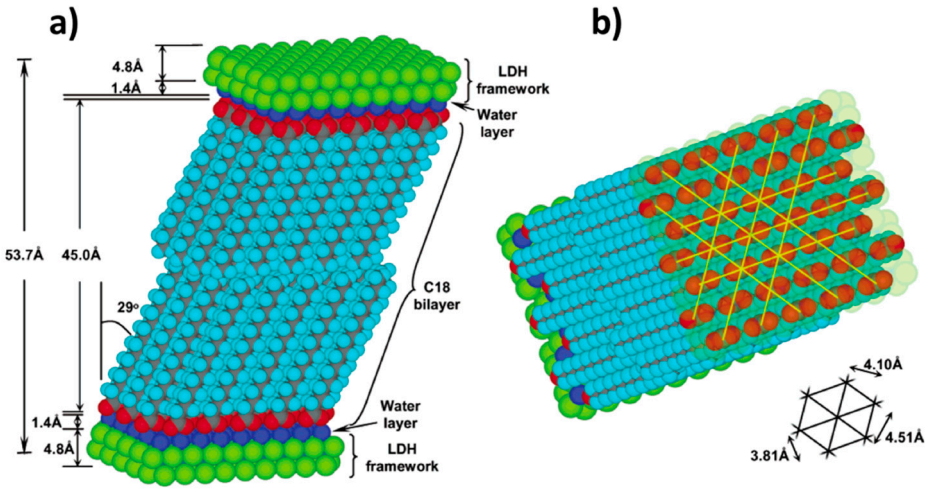


**Figure 4.** Scheme of stearate ions ordered layer assembly into LDH: (**a**) tilted bilayer, and (**b**) packing of stearate ions in the LDH framework. Reprinted with permission from Ref. [94] Copyright (2003) American Chemical Society.

### 3.3. Amino Acids

Amino acid intercalation inside LDHs is also a well-known topic [95]. An interesting application of LDHs-intercalated with amino acids is constituted by drug delivery, specifically because amino acid molecules provide the interaction sites to effectively improve drug-loading [96]. Apart from the interest in elucidating the structural features, the interaction between anionic clays and amino acids is very interesting and may offer an insight into the active role of LDHs in the polymerization of amino acids, in addition to the well-known characterization of the intercalation [95]. Differently from nucleotides, for which the prebiotic synthesis route is still speculative [89], there is a little more evidence of the possibility that amino acids were present in prebiotic systems. Accordingly, both cationic clays and LDHs might have facilitated the polymerization of amino acids, thanks to the possibility to absorb them via their negative C-termini. Interestingly, as argued by Paecht-Horowitz [97], the former can catalyze polymerization only when the amino acid is small enough to enter the interlayer space of the clay. As for the latter, the computational study from Erastova et al. [54] demonstrated the possibility that LDHs could be a functional system for amino acid adsorption and polymerization on the positively charged LDH surface. Intriguingly, all the amino acids they investigated (alanine, aspartate, histidine, leucine, lysine and tyrosine) showed an increase in adsorption upon dehydration,

with the only exception of lysine. Dehydration, in turn, decreases the interlayer spacing, in accord with our experimental findings [37], favoring both the crowing of amino acids and the alignment of the N- and C-termini, and also permitting the formation of a peptide bond (see Figure 5). This reaction leads to the loss of charged group, which, in turn, allows for the introduction of a new amino acid to an adjacent site, where it then can react with the peptide's C-terminus. The growing peptide chain remains tethered at the LDH surface via the C-terminus of the latest amino acid added. Differently to nucleic acids, amino acids do not form strong association on the LDH surface. Even more, the authors observe that, within the clay layers, peptide chains should be able to undergo hydrophobic collapse, an essential mechanism of protein folding, in perfect resemblance to the ribosome systems.

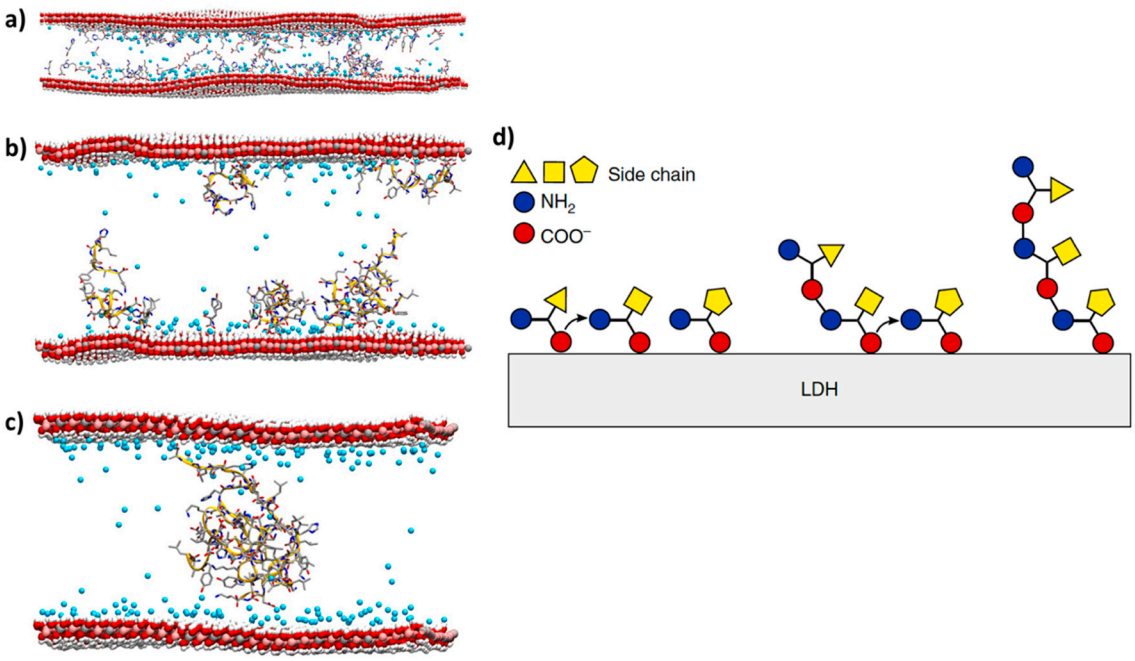


**Figure 5.** Amino acids on LDHs. Ensembles of (**a**) amino acids; (**b**) short; and (**c**) long peptides intercalated into LDH interlayers via their C-terminal. (**d**) Proposed mechanism for peptide bond formation inside LDH interlayers. Reproduced from Ref. [54] under the terms of the Creative Commons CC BY license.

### *3.4. Carbohydrates and Cellulose*

Carbohydrates are among the most abundant biomolecules in nature. They are formed by plants through photosynthesis and serve as energy sources, structural building blocks and biorecognition elements in organisms. They can exist as oligomers and polymers; the latter are formed by linking single monomeric units with glycosidic bonds. LDHs have been leveraged as systems to prepare biomimetic composites with carbohydrates molecules showing enhanced mechanical properties, mimicking the natural structure of nacre, a biological organic–inorganic composite material produced by some mollusks and formed by the ordered stacking of calcium carbonate and crosslinked protein, resulting in very good mechanical properties (high tensile strength, about 150 MPa). To this aim, it is worth mentioning some previous studies on LDH composites with carboxymethyl cellulose (CMC) [98] and cellulose nanofibrils [99], which exhibited improved mechanical properties. As reported in Figure 6a, the interaction of CMC with LDHs is purely electrostatic, being driven by the negative electrostatic charge of the CMC that permits its insertion into MgAl-LDH galleries. In addition, alginate was also used as composite with LDHs [100], following a bioinspired approach that mimicked the mechanical properties of nacre. In particular, NiAl-LDH is prepared by coprecipitation and is subsequently exfoliated mechanically; after that, it is mixed with an alginate solution permitting to

obtain alginate-coated LDH, which is subsequently crosslinked with $Ca^{2+}$ (see Figure 6b). Importantly, the ionic crosslinking of alginate by calcium ions along with the hydrogen bonds between NiAl-LDH and alginate, allows the nacre film to be mimicked, achieving a tensile strength as high as 194 MPa, in addition to transparency higher than 70% in the visible light range.

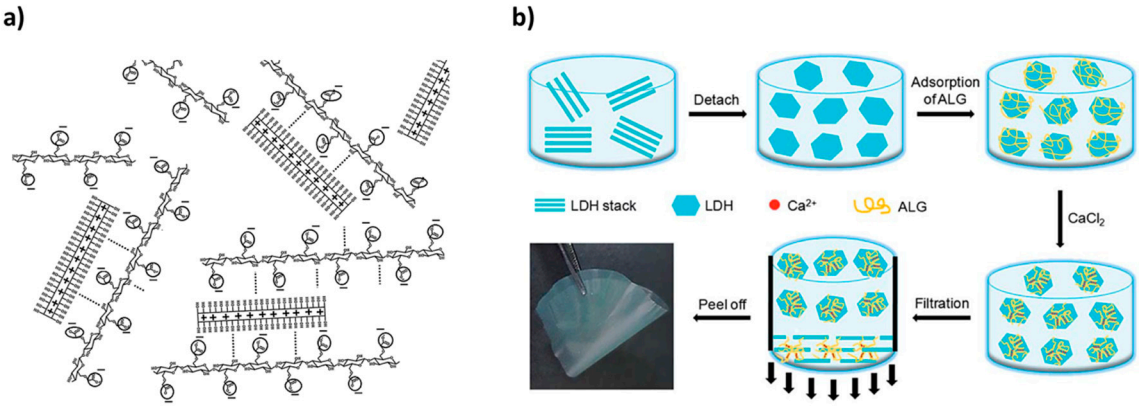


**Figure 6.** (**a**) Stabilization of the MgAl-LDH-CMC hybrid particle by electrostatic-driven interactions. Reprinted from Ref. [98]. Copyright (2014) with permission from Elsevier. (**b**) Production process of hybrid NiAl-LDH/Alginate-$Ca^{2+}$ film. Reproduced from Ref. [100]—Published by The Royal Society of Chemistry.

## 4. Life-like Clays Based Artificial Compartments

The fabrication of artificial compartments that mimic life-like properties is a topic of large interest and has been boosted by the development of new microfluidic platforms containing droplet-based and vesicle-based artificial cells [101,102], and by the employment of printing methodologies, as shown also by our group [103,104]. The systems can be realized at solid surfaces mimicking the processes of DNA condensation [105] or in membrane-enclosed liquid compartments [106,107]. Importantly, such artificial biosystems permit to recapitulate some of the features of primitive sub-micron sized protocells, such as effect of droplet size on the molecular behavior, molecular confinement, molecular crowding, and liquid–liquid phase separation. In the context of clay-based compartments, the studies are mainly based on the fabrication of 100–10 μm sized colloidosomes or Pickering emulsions [108], showing intriguing membrane permeability [109,110], and even some life-like behavior, such as enzyme-powered motility [111]. Regarding the fabrication of synthetic compartments, printing methods are gaining increasing importance [112,113], given their rapidity, low-cost and adaptability to biomolecular, organic and inorganic inks [114] or oil droplets [115], opening up the possibility to print artificial cell-like systems with higher degree of flexibility and possibility to assemble complex predesigned droplet networks. The development of compartments containing LDHs is still at its infancy. However, the possible application of LDH-based compartments would lead to the mimicking of nanocomposites, as for instance mimicking the structure and the mechanical properties of the high strength seashell nacre. A fundamental study by Zhang and Evans [116] explored the dynamic assembly of LDH platelet-rich droplets drying onto solid surfaces, taking into consideration the interplay of capillary flows, colloidal stability and pH on the final CoAl-LDH composite deposited on a silicone coated paper. They prepared pH 3 and 10 dispersions resulting in well-dispersed and flocculated CoAl-LDH platelet suspensions, respectively. The pH-dependent colloidal stability of CoAl-LDH dispersions in the pH range from 3 to 10 was discussed by the same authors in another report [117], showing that the suspension was most stable at pH 3, due to the protonation of the OH groups resulting in repulsion forces between LDH platelets, positively charged on both basal and edge surfaces. It is worth pointing out that both stronger acid and basic conditions (i.e., pH < 3 and pH > 10) lead to LDH structural dissolution [118,119]. In the case of deposition of droplets at pH 3 (where

LDHs are well dispersed), a central hole was observed in the LDH deposit (see Figure 7a), along with a ring of higher thickness at 0.6 *r* from the center (where *r* is the radius of the droplet). The authors explained this structure by considering possible capillary effects between LDH platelets. A completely different situation occurred in the case the LDH platelets were deposited as flocculated at pH 10. In this case, the suspension produced a flatter structure due to the lack of capillary flows. As the authors state, these results could be applied to the understanding of droplet morphologies produced by inkjet printing [120], with the aim to optimize both the flow processes in a drying drop and the stacking interactions among LDHs, ultimately permitting to obtain ordered stacking and high uniformity in the LDH coverage. An elegant demonstration of LDH printing was given by Zhu et al. [121] who leveraged exfoliation processes of CoAl-LDH and NiAl-LDH nanosheets in formamide to obtain printable LDH formulations, leading to stable LDH-based solid films (see Figure 7b), in which the LDH stacking is able to mimic the structures of nacre, potentially leading to good mechanical properties. Notably, the authors also demonstrated the possibility to tune the optical and mechanical properties of the LDH films by tuning the anions that can be stacked into the galleries.

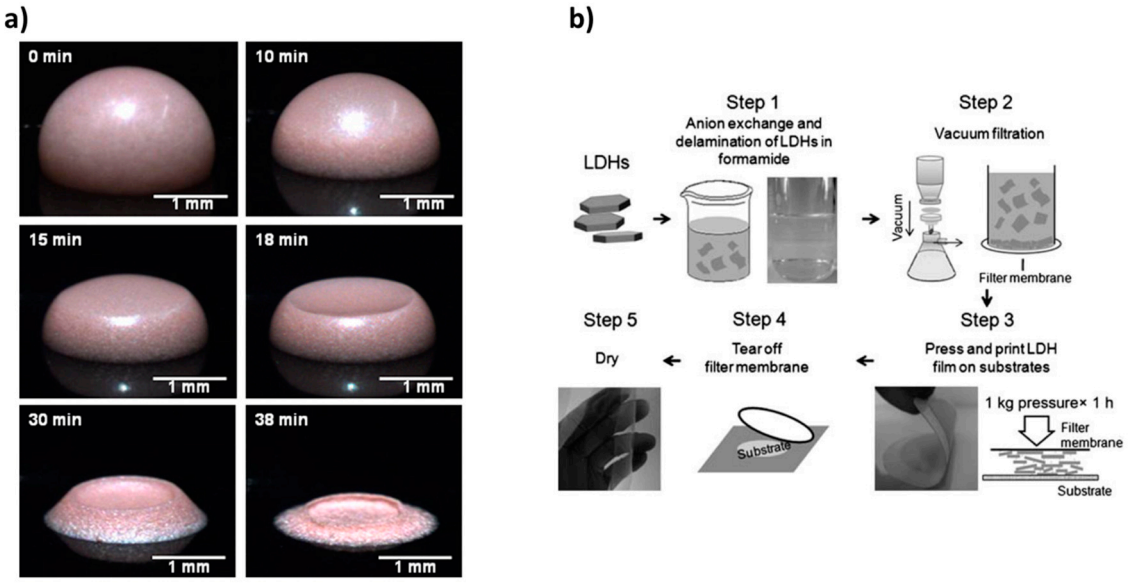


**Figure 7.** (**a**) Photographs of a drying drop of 2.0 vol% LDH dispersion at pH 3 as a function of drying time. Reprinted from Ref. [116]. Copyright (2013) with permission from Elsevier. (**b**) Schematic diagram of the preparation of LDH thin films and subsequent printing on substrates. Reproduced from Ref. [121] with permission from The Royal Society of Chemistry.

## 5. LDH-Bioinspired Devices

### *5.1. Applications in Composites and Coatings*

Billions of years of evolution have produced optimized natural materials with outstanding properties resulting by the combination of organic and inorganic elements, which inspire scientists and engineers to design artificial materials. In recent years, the development of bioinspired composites has become an exciting direction for the fabrication of novel multifunctional materials, which exhibit a combination of outstanding mechanical, fire-shielding, optical and oxygen barrier properties. In this field, LDHs are receiving increasing attention since they offer numerous advantages over other inorganic layered materials, also in the field of nanocomposites [122,123]

Shu et al. [124] reported on a nacre-like film based on heparine/NiAl-LDH with a layered nano/microscale-hierarchical structure fabricated by the vacuum-filtration method (Figure 8a). The realized hybrid film showed a reduced elastic modulus (Er ≈ 23.4 GP) and a hardness (H ≈ 0.27 GPa) remarkably higher than those of other reported polymer/LDH composites. In addition to such

outstanding mechanical characteristics, the LDH composite exhibited interesting UV-blocking, flame retardant, and heat-shielding properties. In a successive work, the same group [125] studied a hierarchical structure based on a CoAl-LDH/Poly(vinyl alcohol) film, prepared for the first time by bottom-up layer by layer assembly (Figure 8b). A combination of high tensile strength and elastic modulus is obtained through an appropriate CoAl-LDH aspect ratio, which well compares to those of nacre and lamellar bone.

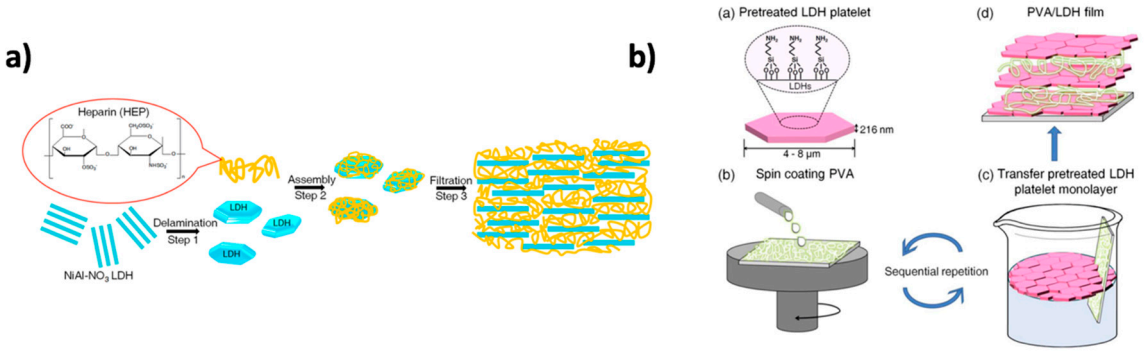


**Figure 8.** (**a**) Fabrication of the artificial nacre-like HEP/LDH film by three steps: (i) LDH delamination; (ii) assembly of exfoliated LDHs and HEP; and (iii) HEP-LDH hybrid building blocks are aligned by self-assembly induced by vacuum filtration. Reproduced with permission from Ref. [124]. Copyright year (2014) American Chemical Society. (**b**) Fabrication of artificial multilayered PVA/LDH hybrid films by: (i) modification of the surface of LDH platelets with slightly hydrophobic amine-terminated APTES; (ii) spin coating of a layer of PVA; (iii) gradual formation of Langmuir film at the air–water interface; and (iv) sequential repetition to fabricate multilayer films. Reproduced with permission from Ref. [125]. Copyright year (2014) American Chemical Society.

Meng et al. [126] reported another example of brick-and-mortar structure to enhance the mechanical performance of a composite. They developed a PTFE/MLDH (modified ZnAl-LDH)/GF (glass fiber) composite inspired by layer–layer structure and prepared via the multi-layered dipping method, which consists of GF acting as a reinforcement, PTFE acting as matrix and MLDH acting as the layer–layer structure. The results show that the tensile strength and the strain value of PTFE/MLDH/GF composites, with MLDH content around 1.6 wt%, increased to 163.57 MPa and 8.33%, respectively. These values resulted better than those of pure PTFE/GF composites, showing a tensile strength of 112.72 MPa and a fracture strain of 4.99%.

Interestingly, the use of LDH-based compounds is not only limited to mechanical properties, as mentioned above. Liu et al. [127] demonstrated that the combination of two or more diverse materials in a unique composite is a winning strategy, realizing a durable superhydrophobic sponge for oil and organic collector with magnetic-responsive and fire retarding properties. To achieve this result, by means of a two-step process, they combined polydopamine (PDA), ZnAl-LDH, $Fe_3O_4$ nanoparticles and n-octadecyl mercaptan (OM), acting, respectively, as a "bio-glue", a fire retardant agent, magnetic material and hydrophobic reagent. First, PDA-modified ZnAl-LDH and $Fe_3O_4$ were anchored on the skeleton of polyurethane (PU) sponge by self-polymerization. Next, OM containing thiol groups were covalently combined with PDA by means of Michael addition reaction. The resulting sponge (Figure 9a,b) exhibited remarkable hydrophobicity (water contact angle of 163°) and highly oleophilic (oil contact angle of 0°). As a result, it could absorb various kinds of oils and organics up to 53.6 times of its own weight, and the absorbed oils could be collected through a simple squeezing process (Figure 9c). In addition, the presence of magnetic material, $Fe_3O_4$, allows easy drive by an external magnetic bar, thus reducing any contaminations.

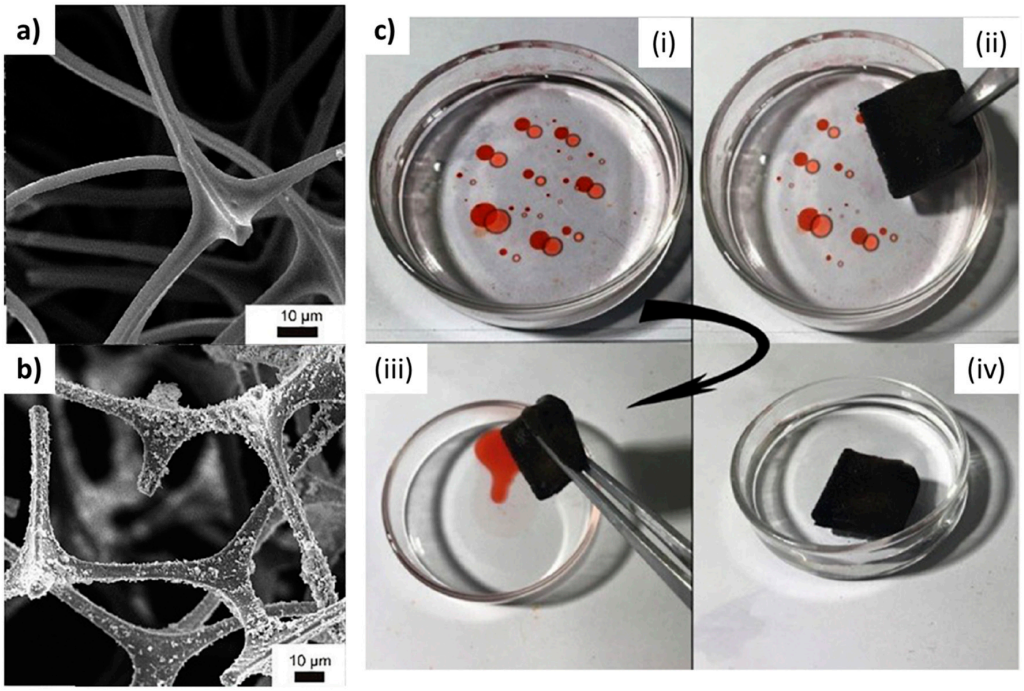


**Figure 9.** (**a**) SEM images of pristine PU sponge, (**b**) SEM images of PU-LDH-$Fe_3O_4$-PDA-OM sponge, (**c**) A series of photographs for the process of absorption and collection toluene (dyed with Sudan III) from the surface of water. Reprinted from Ref. [127] with permission from Elsevier.

The composite materials are also considerably advantageous in the realization of coating films in a large number of fields, leading to an increase in performance and multifunctionality. For example, Wang et al. [128] fabricated superhydrophobic MgAl-LDH coatings on medium density fiberboards with flame retardancy, obtained by the deposition of polydimethylsiloxane (PDMS) and 1H, 1H, 2H, 2H perfluorodecyltrichlorosilane (FDTS)-modified LDH particles. The PDMS@FDTS-Mg/Al LDH coating exhibited superhydrophobicity with a water contact angle of 155° and self-cleaning property. The flame retardant character was evaluated by limiting oxygen index (LOI) and cone calorimeter test. LOI value of superhydrophobic MDFs increased by 60.4% as compared to that of the pristine MDFs, from 24.0 to 38.5. The peak heat release rate (PHRR) and total heat release (THR) of MDFs coated with PDMS@FDTS-Mg/Al LDH reduced by 24.7% and 11.2% as compared to MDFs alone. This result demonstrates that the presence of inorganic coating improved the flame retardancy of the MDFs. Wu et al. [129], inspired by the micro- and nanostructure of lotus leaves, or the Cassie state surface, developed a self-layered coating on magnesium alloy through a hydrothermal treatment, followed by radiofrequency (RF) magnetron sputtering of polytetrafluoroethylene (PTFE). A super-hydrophobic (water contact angle of 170°) and acid resistant surface is created on the alloy. Recently, Yu et al. [130] reported on the possibility to use an environment-friendly LDH-base coating as high oxygen barrier coating in flexible food packaging. The coating film is realized by the reconstruction of MgAl-LDH from MgAl-layered double oxide (LDO) in concentrated aqueous glycine solutions, resulting in a coating solution of LDH and poly(vinyl alcohol) (PVA). It is worth observing the key role of the aspect ratio of reconstructed LDH in the coating permeability performance. Indeed, the relative permeability (P/P0) of the LDH/PVA coated layer decreases as the aspect ratio of LDH nanosheets are increased, from 0.0065 with aspect ratio 87 ± 17 to 0.0038 at 336 ± 170. This is explained by the highest aspect ratio of LDH nanosheets, which leads to better alignment in the coated layer. Thus, through the fine control of aspect ratio, the coating film reached an oxygen transmission rate <0.005 $mL \cdot m^{-2} \cdot day^{-1}$ at a film thickness of 1175 ± 101 nm.

### 5.2. Nanogenerators and Physical Sensors

In the era of smart devices and bioinspired sensor networks, LDHs and related compounds have been demonstrated to play multiple roles, starting, for example, from green nanogenerators for realizing self-powered sensors. In this field, it is worth to mention the work by Cui et al. [131], and those by Sun et al. [132] and Tian et al. [133], who realized a water-driven triboelectric nanogenerator (WD-TENG) and a natural water evaporation (NWE) driven generator, respectively, to harvest energy from water, the most abundant substance on our planet. Briefly, in the first approach, the realization followed a bottom-up strategy, by directly growing a well oriented MgAl-LDH nanosheet network on a metal substrate (Figure 10a). To reduce the surface energy, a further surface modification was performed via crosslinking of fluorine contained silanes, which in turn changed the morphology of the LDH network into a flower-like shape (Figure 10b). The fabricated WD-TENG relied on triboelectric effect, collecting energy from water droplets through the functionalized LDH film as triboelectric layer. The working mechanism is based on a contact-electrification and electrostatic induction at the liquid–solid interface (Figure 10c,d). In the second approach, a NWE-driven generator (NWEG) was realized via a spray-deposition of NiAl-LDHs on a polyethylene terephthalate (PET) substrate [132] (Figure 10e). It operates by means of an NWE-driven gradient of water which flows across the naturally formed surface-charged nanochannels between the LDH flakes, which were evenly spaced on the PET surface, with an ordered layer-by-layer stacking on the substrate (average channel width less than 50 nm) (Figure 10f,g). The performance of the NWEG was reasonably supposed to be regulated by the surface charge density ($d_c$), the hydrophilic character and the presence of nanochannels or pores in the NG active layer, which are easily tunable intrinsic properties in the case of LDHs. In a successive work [133] the same group reported on the relationship between $d_c$ and the NWEG performance by precisely tuning $d_c$ of NiAl-LDHs in the range of 2.52–4.59 e/nm$^2$, by adjusting the molar ratio of $Al^{3+}$ to $Ni^{2+}$.

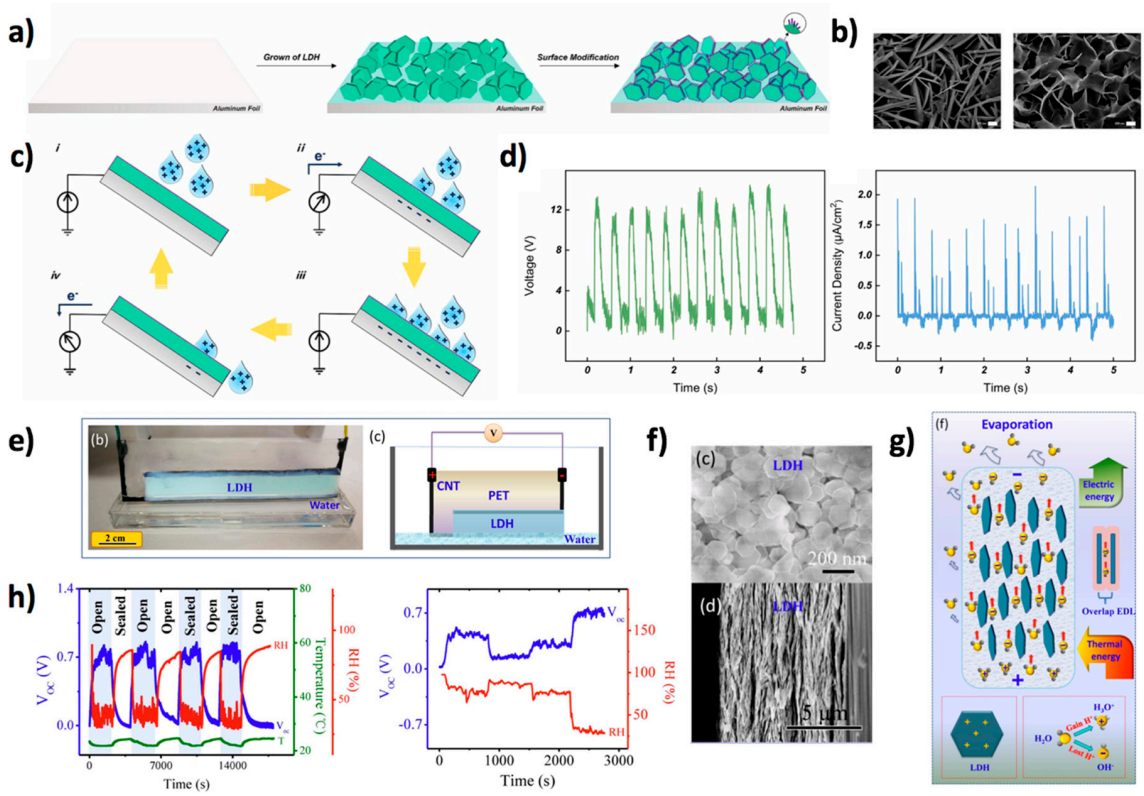


**Figure 10.** LDH-based water driven nanogenerators. (**a**) Schematic illustration of the fabrication process for the LDH-based triboelectric layer of the WD-TENG, showing (from left to right) the bare aluminum foil substrate and the MgAl-LDH nanosheet network before and after surface modification.

(**b**) Scanning electron microscope (SEM) images of the as grown (left) and surface modified (right) LDH film. (**c**) Schematic diagram of the modified LDH- (green) based WD-TENG collecting energy from water droplets. (**d**) Output voltage and current density of the WD-TENG under water droplets impacting. Reproduced from Ref. [131] with permission from Elsevier. (**e**) Photo (left) and schematic illustration (right) of the NiAl-LDH NWEG. (**f**) Top-view (top) and cross-sectional (bottom) SEM images of the NiAl-LDH film. (**g**) Schematic diagram of the working principle of the NWEG on a microscopic level. (**h**) (left) Evolution of the open circuit voltage ($V_{OC}$, blue line) in response to the variation of the relative humidity (RH, red line) due to periodic opening and sealing of the container. (right) Response of $V_{OC}$ to periodic variations of RH between 96% and 28%. Reproduced from Ref. [132] with permission from Elsevier.

Another fundamental element in the fabrication of sensor systems is represented by the energy storage units. In a recent study, Xu et al. [134] reported on the realization of a coplanar asymmetric microscale hybrid device (MHD) supercapacitor based on MXene and CoAl-LDHs using a two-step screen-printing process. The LDH with its faradaic pseudo capacitance behavior was used as positive electrode material to enhance energy density and potential window. The resulting MHD exhibited very interesting electrical properties, such as outstanding cycling stability (92% retention of areal capacitance after 10,000 cycles), potential window extended to 1.45 V, and enhanced energy density (10.80 and 8.84 μWh $cm^{-2}$ in 6 M KOH and with PVA-KOH, respectively). In a more recent work [135], a CoMn-LDH doped with polypyrrole (PPy) was used as positive electrode for asymmetric supercapacitor (ASC) with multilayer graphene as cathode, exhibiting strong electrochemical performance. This supercapacitor showed properties comparable to or better than those of similar devices recently reported, with good cycle performance (99.5% retention after 8000 cycles) and energy density as high as 29.6 Wh $kg^{-1}$ at a power density of 0.5 kW $kg^{-1}$.

The application of LDH in the field of bioinspired sensors was successfully demonstrated by Ren et al. [136], who developed a skin-inspired sensor based on a multifunctional nanocomposite hydrogel consisting of sodium alginate/sodium polyacrylate/layered rare-earth hydroxide (LRH) (SA/PAAS/LRH), fabricated through a 3D printing system (Figure 11a,b). The device showed a promising multifunctional behavior, such as humidity-dependent electromechanical properties, a sensitivity to mechanical deformation, thanks to a strain-dependent conductivity (Figure 11c), and tunable fluorescence (Figure 11d), while maintaining the characteristics of transparency and stretchability indispensable for the realization of a device for human motion detection. Such versatility makes it a good candidate for future soft wearable equipment. The use of LDH was also demonstrated to drastically improve the performance of composite materials for sensors. For example, Beigi et al. [137] reported on a modified ionic polymer metal composite (IPCM) humidity-sensor based on a nafion polymeric matrix doped with CoAl-LDH nanoparticles, with a significant improvement of sensitivity and responsivity due to the intrinsic hydrophilic characteristic of LDH.

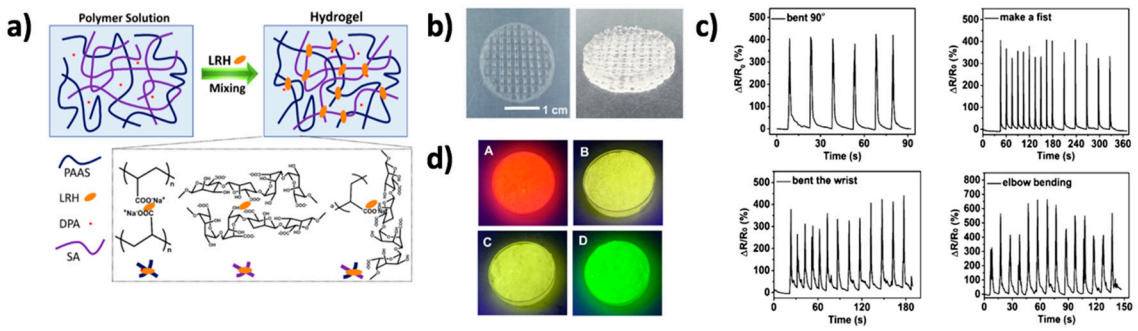


**Figure 11.** Skin-inspired multifunctional device. (**a**) Scheme of the preparation of SA/PAAS/LRH hydrogel. (**b**) Top and side photos of the printed hydrogel wafer with a grid structure. (**c**) Response to

sensor strain. First row: Sensor attached on the forefinger of a human hand responding to bending angles from 0° to 90° (left); and sensor attached on the back of the hand responding when making a fist (right). Second row: Relative changes of the hydrogel films in sensing wrist bending (left); and elbow bending (right). (**d**) Fluorescent colors of various hydrogels, with different rare-earth ratios, under 254 nm in wavelength ultraviolet irradiation. Reprinted with permission from Ref. [136] Copyright (2020) American Chemical Society.

### *5.3. Applications in Oxygen Evolution Reaction*

The process of oxygen evolution reaction (OER), $4\,OH^- + \text{energy} \rightarrow O_2 + 2H_2O + 4e^-$, is one of the most critical steps of electrochemical water splitting, which is widely recognized as a promising and sustainable method to convert the intermittent electrical energy from the nature into stable and storable energy (hydrogen) [138,139]. However, OER, which is a multistep $4e^-$ process, is thermodynamically not favored and thus kinetically sluggish [140]. Indeed, an OER catalyst should be able to overcome both the activation energy barrier ($E_a$) and the standard free energy charge ($\Delta G^0 = 1.23$ eV). In recent years, substantial research efforts have been devoted to develop novel non-noble metal-based active OER catalysts based on efficient, low-cost and earth-abundant substitutes for conventionally used precious metal compounds [141]. Different strategies have been conceived to improve the catalyst performance, which may be categorized on three scale levels [142]: (i) at the atomic-scale (e.g., alteration of oxidation state, doping, coordination and composition of metal composites); (ii) at the nano-scale, including different material combinations templated on nanostructures (e.g., nanowires, nanosheets and nanotubes), to increase OER activity by means of high surface area and number of active sites; and (iii) at the meso-scale, i.e., the creation of a porous supporting architecture to enhance mass transport to electrolytes and structural stability. As intriguingly noted in recent studies [142–144] such optimization problem presents many analogies with the demand of photosynthesis in the evolutionary development of plant leaves, like the need of maximized surface area to capture as much light as possible, and sufficient space between neighbors to promote good gas exchange and surface reactions. In addition the 1D hollow tubular structures under the leaves facilitate the transport of nutrients and water to each leaf [142].

In the last decade, LDHs have been proven to be highly active, cost-effective and durable OER catalysts, exhibiting electrocatalytic activity and stability for OER, comparable to or higher than commercial precious metal-based catalysts [145–147]. In their reports, the scholars leveraged all the above-mentioned optimization routes to improve OER activity of LDHs. In particular, in 2014, Lu et al. developed OER electrodes based on a three-dimensional (3D) porous film of vertically aligned NiFe-LDH nanoplates loaded on a nickel foam. Excellent OER performance was demonstrated, with a small onset overpotential (~230 mV), large anodic current density (30 mA $cm^{-2}$) and outstanding electrochemical durability, benefiting from the intrinsic high activity of the NiFe-LDH catalyst [148] and the unique 3D architecture, whose surface area was increased by the highly porous nickel foam. In the following, many research efforts were focused to improve the OER activity of LDHs (typically NiFe- and NiCo-LDHs), as increasing the number of active sites as well as increasing the activity of the individual active site. Song and Hu [149] and Liang et al. [150] demonstrated that liquid exfoliation of LDHs to single-layer nanosheets leads to greatly enhanced OER activity, due to an increase in the number of active edges sites and higher electronic conductivity, while preserving material composition. Next, Wang et al. [151] demonstrated that dry exfoliation of bulk CoFe LDHs into ultrathin LDH nanosheets through Ar plasma etching also resulted in the formation of multiple vacancies (including O, Co and Fe vacancies), thereby producing a dual effect to OER enhancement, due to the great number of exposed active sites in the 2D LDH nanosheets and their improved activity due to multiple vacancies. The dry-exfoliated CoFe-LDH performed very well in the OER with an overpotential of 266 mV to reach a current density of 10 mA $cm^{-2}$ vs. 321 mV required for the untreated pristine CoFe-LDH. In a further report, the same group [152] dry-exfoliated bulk CoFe-LDHs in a $N_2$ plasma into edge-rich ultrathin nanosheets featuring, again, multiple vacancies, as well as nitrogen doping, which facilitated absorption of OER intermediates by altering the electronic density of the adjacent Co or Fe atoms.

The ultrathin N-doped CoFe LDH nanosheets loaded on Ni foam exhibited excellent OER performance, with an overpotential of 233 mV at a current density of 10 mA $cm^{-2}$. However, despite such atomic- to nano-scale optimization strategies, the OER performance of LDHs was limited by their intrinsically poor electrical conductivity. Some reports have proposed combining LDHs with conducive materials, e.g. carbon nanotubes [153], graphene [154], graphene oxide [155] and, more recently, silver [156] and CuO nanowires [157]. As for the latter, inspired by the monocot leaf structure in nature, Chen and coworkers conceived an engaging biomimetic nanoleaf based on ultrathin NiCo-LDH nanosheets in situ grown on Cu nanowires, forming a NiCo-LDH lamina featuring large electrochemical surface area (ECSA) and numerous active edge sites for OER reaction (see Figure 12). The CuO nanowires served as veins to support the LDH lamina, while providing mechanical support as well as improving the LDH conductivity, further increasing the OER activity. An enhanced OER performance was then achieved, significantly improved with respect to that of conventional NiCo-LDHs, with a quite small overpotential of 262 mV at 10 mA $cm^{-2}$, good stability and flexibility.

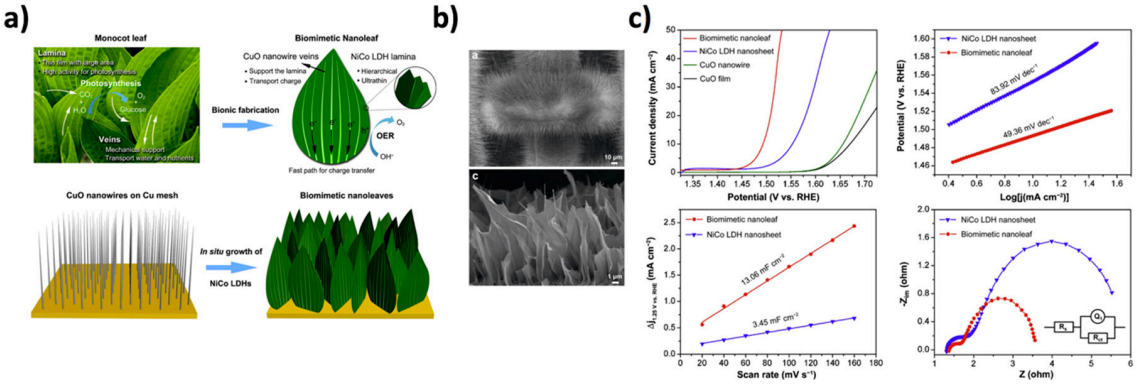


**Figure 12.** Biomimetic LDH nanoleaf for OER. (**a**) Schematic illustration of the biomimetic NiCo-LDH based nanoleaf, showing (top) a photograph of the monocot leaf and a sketch of the biomimetic nanoleaf, with indication of the OER process, and (bottom) the fabrication procedure, with in situ growth of NiCo-LDH on the CuO nanowires/Cu mesh substrate. (**b**) SEM images of the CuO nanowires on the Cu mesh (upper panel, scale bar 10 μm), and of the biomimetic nanoleaves (bottom) (scale bar 1 μm). (**c**) OER performance. First row: Linear sweep voltammetry (LSV) polarization curves (left); and corresponding Tafel plots (right). Second row: Capacitive current vs. scan rates (left); and Nyquist plots at an overpotential of 300 mV (0.1 Hz to 100 kHz) (right). Reprinted from Ref. [157] with permission from Elsevier.

### *5.4. Peroxidase-Like Activity*

The peroxidase enzymes are widespread in natural systems from bacteria to plants and humans, given their fundamental role in decomposing hydrogen peroxide ($H_2O_2$), which is a toxin produced as a byproduct of oxygen during aerobic respiration processes. These proteins contain a heme group in their active site that uses hydrogen peroxide as the electron acceptor to catalyze oxidative reactions. Such electron transfer ability between reducing substrate and $H_2O_2$ can be conveniently mimicked by many metal oxide nanoparticles—e.g., iron oxides, cerium oxides, metal sulfides and carbon nanodots. In this regard, many reports have focused on the realization of hybrid structures in which LDHs increase the surface/volume ratio and favor the dispersion of the nanoparticles, thereby allowing the peroxidase activity to be enhanced, as demonstrated by Yang et al. with CoAl-LDH/$MFe_2O_4$ (M = Ni, Zn, Co) [158] or CoFe-LDH/$CeO_2$ hybrids [159], as well as core–shell $Fe_3O_4$/CoFe-LDH [160], finding applications in the field of analytical chemistry, especially for the determination of glucose, $H_2O_2$ and glucose and ascorbic acid, respectively. The mechanism of reaction is based on the electron transfer from the molecule 3,3′,5,5′-tetramethylbenzidine (TMB) to $H_2O_2$. In the presence of glucose oxidase enzyme, glucose is oxidized to gluconolactone and oxygen is reduced to $H_2O_2$. As a result, the higher

is the glucose concentration, the higher is the concentration of $H_2O_2$ and, hence, the amount of oxidized TMB. Conversely, ascorbic acid is able to convert the oxidized form TMB to the reduced state. As a result, the obtained sensor is based on a colorimetric readout (see Figure 13a) and can be effectively employed in the field of low-cost glucose sensing.

Interestingly, LDH materials with intrinsic peroxidase activity were also engineered by simply introducing metal species featuring peroxidase-like activity mimicking the natural heme group. The first examples of such bioinspired systems were shown by Zhang et al. [161] who leveraged CoFe-LDH nanoplates to obtain a colorimetric sensor for $H_2O_2$ (based on the oxidation of TMB), reaching the optimal detection limit of 0.6 μM. Other similar examples are those from Su et al. [162], who leveraged NiCo-LDHs for acetylcholine detection (limit of detection equal to 1.62 μM), and from Zhan et al. [163], who investigated NiFe-LDHs as a sensor for $H_2O_2$, reaching the limit of detection of 4.4 ± 0.2 μM (see Figure 13b). Along with colorimetric detection, electrochemistry can also be applied to improve the detection limit of the sensor. In this regard, an example of an electrochemical sensor based on peroxidase mimicking LDHs worth mentioning was recently shown by Fazli et al. [164], who fabricated a PdAl-LDH/carboxymethyl cellulose (CMC) nanocomposite (CMC@Pd/Al-LDH) on a glassy carbon electrode to realize a sensor for $H_2O_2$ (limit of detection equal to 0.3 μM). Interestingly, this work shows how CMC is suitable for improving the sensitivity and the exposed active surface area, finally enabling a high number of available sites for electrochemical reactions. An intriguing application of peroxidase mimics for sensing acetylcholine (limit of detection equal to 1.7 μM) was reported by Wang et al. [165] who prepared NiAl-LDH/Carbon dot nanocomposites onto glassy carbon electrodes.

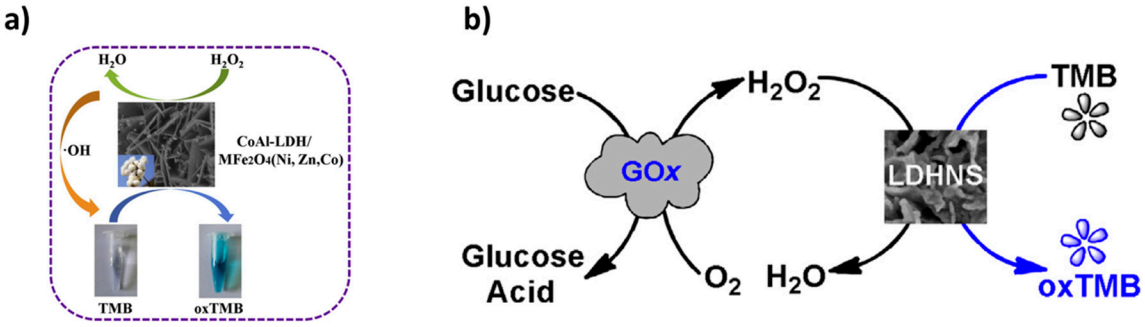


**Figure 13.** LDH-based peroxidase mimics. (**a**) CoAl-LDH/$Fe_2O_4$ hybrid materials catalyze the oxidation of TMB in presence of $H_2O_2$, mimicking the peroxidase activity. Reprinted from Ref. [158] with permission from Elsevier. (**b**) Intrinsic peroxidase-like activity in NiFe-LDH can be leveraged to build up colorimetric sensors for $H_2O_2$ and glucose. Reprinted from Ref. [163] with permission from Elsevier.

### *5.5. LDHs on Biotemplates for Bioremediation*

The intrinsically high surface to volume ratio of LDHs, possibly enhanced by recently proposed ultrathin LDH synthesis routes [166–168], has been leveraged for many applications that require physical processes of absorption and interaction with molecules for bioremediation of contaminated sites, such heavy metals, toxic substances, pesticides or even favoring their photo-induced degradation [169]. An approach for further improving the efficiency of LDH-empowered devices for bioremediation is the realization of 3D biomimetic structures or the coupling with organic biotemplates (typically of plant origin) aiming at the realization of life-mimicking 3D high-surface hierarchical organization, miniaturization, eco-friendly characteristics and even specificity for the absorption of targeted molecular systems. For instance, typical examples of biotemplates are constituted by diatomaceous earth, leaves and cellulose fibers, which are prone to be easily functionalized by surface functionalization with LDHs.

A plethora of research efforts have been focused on the removal of oil, metal ions, pesticides and agrochemicals from contaminated water by using this combined approach. An interesting example comes from the research of Zhu et al. who showed a one-step synthesis of a biomimetic cactus-like

hierarchical architecture for oil/water separation [170], based on a CoNi-LDH coated stainless steel mesh. The role of the 3D LDH morphology appears to be the key factor to induce an outstanding water locking capability into the cactus-like hierarchical structure. The trapped water is, in turn, able to form a stable water layer on the surface, ultimately forming a bioinspired barrier against oil penetration into the mesh, since the resulting surface would be superhydrophilic and underwater superoleophobic. The authors tested different types of oils (diesel oil, lubricating oil, silicon and n-hexane), finding excellent oil rejection ratio and high separation capability and outstanding recyclability over 20 cycles.

Abolghasemi and coworkers used the hierarchical structure of boehmite decorated with MgAl-LDH and porous carbon on a steel fiber for solid phase microextraction of fifteen different pesticides [171]. Interesting examples have also been provided for the removal of Congo red (CR), a dye which is widely employed in many textiles and biotechnological based industries. MgAl-LDH modified diatoms [172] and bioinspired magnetic $ZnFe_2O_4$ microspheres synthetized using pine pollen and covered with MgAl-LDH [173] have been used with this purpose. The presence of LDH significantly improved the absorption capacity of the composite material toward the dye, reaching values of about 300 mg/g in both cases. Whereas the 3D structure of the diatom triggered a multilayer CR dye adsorption, in the case of the magnetic $ZnFe_2O_4$ microspheres, the adsorption was better fitted following a Langmuir model. A very clever bioinspired approach for CR and Doxycycline (DC) removal and photodegradation under simulated sun light irradiation was proposed by Bing et al. [174], who combined photoactive bismute oxides, MgAl-LDH synthesized onto lotus pollen used as template, and calcination (C) treatments, for the fabrication of $Bi_2O_3/Bi_2WO_6$/MgAl-CLDH heterojunction hybrids with a 3D hierarchically porous structure. The adsorption of both CD and DC was very efficient, reaching 205.3 and 204.3 $mg{\cdot}g^{-1}$, respectively. Another relevant application of LDH triggered bioremediation comes from the examples in which toxic heavy metals ions can be absorbed on the LDH surfaces. To this aim, NiFe-LDHs [175] have been shown in combination with graphene oxide nanocomposite for the efficient removal of Pb(II) and Cd(II) ions from water, obtaining a maximum adsorption capacity of 986 and 971 $mg{\cdot}g^{-1}$, respectively, following a Langmuir model. A truly bioinspired system that efficiently removes $Cu^{2+}$ ions is the one shown by Dou et al. [176]. The authors leveraged functionalization of MgAl-LDH surface by using the Kabachnik–Fields reaction. More specifically, the MgAl-LDHs were modified with polydopamine, which was further used as source of reactive amino groups used for functionalization with diethyl phosphite, terephthalaldehyde and thiourea, finally allowing the introduction of phosphate groups in the LDHs which are able to specifically adsorb $Cu^{2+}$ ions, up to 105.44 $mg{\cdot}g^{-1}$. In another interesting report, Wang et al. [177] prepared a hybrid material that combined sulfide (derived from $(NH_4)_2MoS_4$) intercalated NiFe-LDHs with alginate for the extraction of $Pb^{2+}$ in aqueous environments. The authors combined the high surface/volume ratio of the bioinspired alginate hydrogel with the LDH sulfide specific interaction with $Pb^{2+}$, leading to maximum adsorption capacity of about 18 $mg{\cdot}g^{-1}$.

An outstanding bioinspired example of phosphate removal from water was shown by Lai et al. [178] who prepared a highly porous composite combining graphene oxide/MgMn-LDH (GO/MgMn-LDH) onto *Garcinia subelliptica* leaves, that constituted a natural bio-template (see Figure 14). The authors grew MgMn-LDH in-situ on the leaf-templated GO (L-GO) to obtain L-GO/MgMn-LDH. Interestingly, after calcination at 300 °C (L-GO/MgMn-LDH-300), the flavonoids which derived from the leaves were able to intercalate into the LDHs, avoiding the collapse of its structure. In addition, these biomolecules provided an outstanding specificity towards the interaction with phosphate ions, which was quantified as 244.08 $mg{\cdot}g^{-1}$ at pH 3. The phosphate adsorption was very much dependent on the pH. Whereas optimal values were obtained at acidic pHs, the higher was the pH, the higher became the competition between $OH^-$ groups and phosphate in the interaction with the LDHs, finally reducing the efficiency in phosphate adsorption. Another clever example of biotemplated approach for the removal of antibiotic, i.e., doxycycline, from water was shown by the intriguing approach of Bing et al. [179] who realized 3D hierarchical tubular micromotors from kapok fibers which were functionalized with Br-intercalated MgAl-LDH/$Mn_3O_4$ hybrid. The manganese oxide permitted to

catalyze $H_2O_2$ decomposition generating oxygen bubbles for self-propulsion. The $Br^-$ anions acted as initiator to form an imprinted polymer to specifically absorb doxycycline up to 224.23 $mg \cdot g^{-1}$.

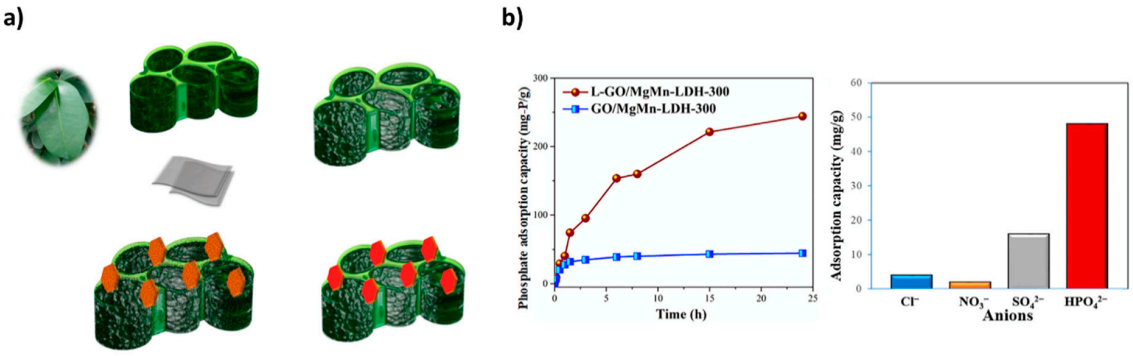


**Figure 14.** *Garcinia subelliptica* leaves templates for GO/MgMn-LDH based removal of phosphate anions. (**a**) Scheme of the templated assembly. (**b**) Phosphate anion adsorption capacity of L-GO/MgMn-LDH-300 compared to that of the calcined LDH composite without leaf-template (GO/MgMn-LDH-300) (left) and anion selectivity of L-GO/MgMn-LDH-300 (right). Figure reprinted from Ref. [178] with permission from Elsevier.

## 6. Conclusions and Perspectives

The field of LDHs is rapidly evolving from the initial investigations dealing with the materials discovery for new applications in chemistry, materials science and biomedicine. In fact, leveraging their outstanding simplicity in the synthesis, low cost, reusability and biocompatibility, LDHs have already proved to be a key player for in the field of nanotechnology.

Given their extraordinarily combination of properties and biocompatibility, as well as their capability to catalyze reactions under prebiotic conditions, LDH clays might be a material chosen by the molecular evolution of living systems. However, the approach correlating the existence of LDHs with the origin of life is very bold, and the question whether there could be a relationship between LDH clays (including green rust) and prebiotic synthesis remains unclear, thus continues being a hypothesis that would need to be addressed in depth in future studies. In general, it is believed that clays have been key systems for the development of prebiotic conditions, given their ability in concentrating and protecting life-essential molecules, creating autonomous semipermeable compartments, as well as catalyzing polymerization reactions. In this context, the specific role of LDHs is still underestimated, but it is growing steadily, especially considering the relevant role of these materials in the context of prebiotic peptides synthesis. Motivated by this, the review analyzes the currently state of the art concerning the interactions of life-relevant molecules (DNA, phospholipids, amino acids and carbohydrates) with LDHs, focusing on the structural point of view, in particular analyzing the possible formation of ordered and crystalline systems and, if possible, providing some insights into relevant biological role. Then, after briefly describing the fabrication of LDHs-based life-mimicking compartments, the review focuses on the technologically relevant applications of life-like and life-inspired devices. More specifically, we focus our attention on important applications where bioinspired LDHs play an important role, i.e., composites and coatings, physical and chemical sensors, catalysis and bioremediation.

The low cost and the eco-friendly synthetic approaches for LDHs make them suitable materials for relevant applications, as the formulation of paints, flame retardants, phytosanitary and pharmaceutical products, given their key role as dispersing or encapsulation agents for anionic molecular systems. To our knowledge, Kyowa Chemical Industry was the first to produce synthetic LDHs, since 1966, among their vast product portfolio, obtaining a good market success, especially in the field of resin stabilizers, residual catalyst removal and chlorine absorbers. The path to bring to the market the innovations and approaches reviewed in the present work is clearly challenging, and still many efforts

are requested of researchers to facilitate a more extended development at a larger industrial scale. As a matter of fact, today, many hybrid organic–inorganic nanomaterials are entering a variety of markets [180]. New materials must aim toward higher levels of sophistication, be recyclable and environmentally-friendly and consume less energy or enable energy harvesting. We hope that the bioinspired approach showed in this review could trigger further technological transfer from academia to the industry, highlighting how bio-friendly LDH products can tackle the need of sustainable chemistry approaches for product manufacturing.

This review does not pretend to cover all the possible literature actually available in the field; however, it can be considered as an effort to review the most recent and exciting advancements in the field of bioinspired applications of LDHs. We hope that it can trigger future LDH-based studies, both on the fundamental science and on the applications, with the ultimate aim to favor a further development of LDHs-based nanotechnology under a novel eco-friendly, bioinspired perspective.

**Author Contributions:** Methodology, G.A. and R.P.; writing—original draft preparation, G.A. and G.P.; writing—review and editing, G.A. and G.P.; and supervision, G.A., G.P. and P.G.M. All authors have read and agreed to the published version of the manuscript.

**Funding:** The article processing charges were funded by SIMITECNO SRL, Sistemi e misure per tecnologie, Via Gallian, 62, 00133 Roma (www.simitecno.com).

**Acknowledgments:** We acknowledge the Università degli Studi di Palermo for hospitality and support.

**Conflicts of Interest:** The authors declare no conflict of interest.

## References

1. Laipan, M.; Yu, J.; Zhu, R.; Zhu, J.; Smith, A.T.; He, H.; O'Hare, D.; Sun, L. Functionalized layered double hydroxides for innovative applications. *Mater. Horiz.* **2020**, *7*, 715–745. [CrossRef]
2. Cavani, F.; Trifirò, F.; Vaccari, A. Hydrotalcite-type anionic clays: Preparation, properties and applications. *Catal. Today* **1991**, *11*, 173–301. [CrossRef]
3. *Layered Double Hydroxides: Present and Future*; Rives, V., Ed.; Nova Science Publishers: Huntington, NY, USA, 2001; ISBN 978-1-59033-060-9.
4. *Layered Double Hydroxides*; Duan, X.; Evans, D.G., Eds.; Structure and Bonding; Springer-Verlag: Berlin/Heidelberg, Germany, 2006; Volume 119, ISBN 978-3-540-28279-2.
5. Arrabito, G.; Bonasera, A.; Prestopino, G.; Orsini, A.; Mattoccia, A.; Martinelli, E.; Pignataro, B.; Medaglia, P.G. Layered Double Hydroxides: A Toolbox for Chemistry and Biology. *Crystals* **2019**, *9*, 361. [CrossRef]
6. Choy, J.-H.; Park, M. Cationic and Anionic Clays for Biological Applications. In *Interface Science and Technology*; Wypych, F., Satyanarayana, K.G., Eds.; Elsevier: Amsterdam, The Netherlands, 2004; Volume 1, pp. 403–424, ISBN 1573-4285.
7. Taviot-Guého, C.; Prévot, V.; Forano, C.; Renaudin, G.; Mousty, C.; Leroux, F. Tailoring Hybrid Layered Double Hydroxides for the Development of Innovative Applications. *Adv. Funct. Mater.* **2018**, *28*, 1703868. [CrossRef]
8. Mohapatra, L.; Parida, K.M. A Review on Recent Progress, Challenges and Perspective of Layered Double Hydroxides as Promising Photocatalysts. *J. Mater. Chem. A* **2016**, *4*, 10744–10766. [CrossRef]
9. Costantino, U.; Leroux, F.; Nocchetti, M.; Mousty, C. LDH in Physical, Chemical, Biochemical, and Life Sciences. In *Developments in Clay Science*; Elsevier: Amsterdam, The Netherlands, 2013; Volume 5, pp. 765–791, ISBN 978-0-08-099364-5.
10. Cui, J.; Li, Z.; Liu, K.; Li, J.; Shao, M. A bifunctional nonenzymatic flexible glucose microsensor based on CoFe-Layered double hydroxide. *Nanoscale Adv.* **2019**, *1*, 948–952. [CrossRef]
11. Kura, A.U.; Hussein, M.Z.; Fakurazi, S.; Arulselvan, P. Layered double hydroxide nanocomposite for drug delivery systems; bio-distribution, toxicity and drug activity enhancement. *Chem. Cent. J.* **2014**, *8*, 47. [CrossRef]
12. Da Costa Fernandes, C., Jr.; Pinto, T.S.; Kang, H.R.; Magalhães Padilha, P.; Koh, I.H.J.; Constantino, V.R.L.; Zambuzzi, W.F. Layered Double Hydroxides Are Promising Nanomaterials for Tissue Bioengineering Application. *Adv. Biosyst.* **2019**, 1800238. [CrossRef]

13. Mishra, G.; Dash, B.; Pandey, S. Layered double hydroxides: A brief review from fundamentals to application as evolving biomaterials. *Appl. Clay Sci.* **2018**, *153*, 172–186. [CrossRef]
14. Lu, P.; Liu, Y.; Zhou, T.; Wang, Q.; Li, Y. Recent advances in layered double hydroxides (LDHs) as two-dimensional membrane materials for gas and liquid separations. *J. Membr. Sci.* **2018**, *567*, 89–103. [CrossRef]
15. Forano, C.; Bruna, F.; Mousty, C.; Prevot, V. Interactions between Biological Cells and Layered Double Hydroxides: Towards Functional Materials. *Chem. Rec.* **2018**, *18*, 1150–1166. [CrossRef]
16. Wang, J.; Zhang, T.; Li, M.; Yang, Y.; Lu, P.; Ning, P.; Wang, Q. Arsenic removal from water/wastewater using layered double hydroxide derived adsorbents, a critical review. *RSC Adv.* **2018**, *8*, 22694–22709. [CrossRef]
17. Errico, V.; Arrabito, G.; Plant, S.R.; Medaglia, P.G.; Palmer, R.E.; Falconi, C. Chromium inhibition and size-selected Au nanocluster catalysis for the solution growth of low-density ZnO nanowires. *Sci. Rep.* **2015**, *5*, 12336. [CrossRef] [PubMed]
18. Arrabito, G.; Errico, V.; Zhang, Z.; Han, W.; Falconi, C. Nanotransducers on printed circuit boards by rational design of high-density, long, thin and untapered ZnO nanowires. *Nano Energy* **2018**, *46*, 54–62. [CrossRef]
19. Bukhtiyarova, M.V. A review on effect of synthesis conditions on the formation of layered double hydroxides. *J. Solid State Chem.* **2019**, *269*, 494–506. [CrossRef]
20. Pushparaj, S.S.C.; Forano, C.; Prevot, V.; Lipton, A.S.; Rees, G.J.; Hanna, J.V.; Nielsen, U.G. How the Method of Synthesis Governs the Local and Global Structure of Zinc Aluminum Layered Double Hydroxides. *J. Phys. Chem. C* **2015**, *119*, 27695–27707. [CrossRef]
21. Jose, N.A.; Zeng, H.C.; Lapkin, A.A. Hydrodynamic assembly of two-dimensional layered double hydroxide nanostructures. *Nat. Commun.* **2018**, *9*, 4913. [CrossRef]
22. Bravo-Suárez, J.J.; Páez-Mozo, E.A.; Oyama, S.T. Review of the synthesis of layered double hydroxides: A thermodynamic approach. *Quím. Nova* **2004**, *27*. [CrossRef]
23. Tokudome, Y.; Morimoto, T.; Tarutani, N.; Vaz, P.D.; Nunes, C.D.; Prevot, V.; Stenning, G.B.G.; Takahashi, M. Layered Double Hydroxide Nanoclusters: Aqueous, Concentrated, Stable, and Catalytically Active Colloids toward Green Chemistry. *ACS Nano* **2016**, *10*, 5550–5559. [CrossRef]
24. Kayano, M.; Ogawa, M. Preparation of Large Platy Particles of Co-Al Layered Double Hydroxides. *Clays Clay Miner.* **2006**, *54*, 382–389. [CrossRef]
25. Ma, R.; Liu, Z.; Li, L.; Iyi, N.; Sasaki, T. Exfoliating layered double hydroxides in formamide: A method to obtain positively charged nanosheets. *J. Mater. Chem.* **2006**, *16*, 3809–3813. [CrossRef]
26. Wang, Q.; O'Hare, D. Recent Advances in the Synthesis and Application of Layered Double Hydroxide (LDH) Nanosheets. *Chem. Rev.* **2012**, *112*, 4124–4155. [CrossRef] [PubMed]
27. Liu, Z.; Ma, R.; Osada, M.; Iyi, N.; Ebina, Y.; Takada, K.; Sasaki, T. Synthesis, Anion Exchange, and Delamination of Co−Al Layered Double Hydroxide: Assembly of the Exfoliated Nanosheet/Polyanion Composite Films and Magneto-Optical Studies. *J. Am. Chem. Soc.* **2006**, *128*, 4872–4880. [CrossRef]
28. Liang, J.; Ma, R.; Iyi, N.; Ebina, Y.; Takada, K.; Sasaki, T. Topochemical Synthesis, Anion Exchange, and Exfoliation of Co−Ni Layered Double Hydroxides: A Route to Positively Charged Co−Ni Hydroxide Nanosheets with Tunable Composition. *Chem. Mater.* **2010**, *22*, 371–378. [CrossRef]
29. Carrasco, J.A.; Harvey, A.; Hanlon, D.; Lloret, V.; McAteer, D.; Sanchis-Gual, R.; Hirsch, A.; Hauke, F.; Abellán, G.; Coleman, J.N.; et al. Liquid phase exfoliation of carbonate-intercalated layered double hydroxides. *Chem. Commun.* **2019**, *55*, 3315–3318. [CrossRef] [PubMed]
30. Hibino, T.; Kobayashi, M. Delamination of layered double hydroxides in water. *J. Mater. Chem.* **2005**, *15*, 653–656. [CrossRef]
31. Wang, J.; Bao, W.; Umar, A.; Wang, Q.; O'Hare, D.; Wan, Y. Delaminated Layered Double Hydroxide Nanosheets as an Efficient Vector for DNA Delivery. *J. Biomed. Nanotechnol.* **2016**, *12*, 922–933. [CrossRef]
32. Zhang, Z.; Min, L.; Chen, P.; Zhang, W.; Wang, Y. Nature-inspired delamination of layered double hydroxides into monolayered nanosheets in water. *Mater. Lett.* **2017**, *195*, 198–200. [CrossRef]
33. Wang, Q.; O'Hare, D. Large-scale synthesis of highly dispersed layered double hydroxide powders containing delaminated single layer nanosheets. *Chem. Commun.* **2013**, *49*, 6301–6303. [CrossRef]
34. Ruengkajorn, K.; Erastova, V.; Buffet, J.-C.; Greenwell, H.C.; O'Hare, D. Aqueous immiscible layered double hydroxides: Synthesis, characterisation and molecular dynamics simulation. *Chem. Commun.* **2018**, *54*, 4394–4397. [CrossRef]

35. Guo, X.; Xu, S.; Zhao, L.; Lu, W.; Zhang, F.; Evans, D.G.; Duan, X. One-Step Hydrothermal Crystallization of a Layered Double Hydroxide/Alumina Bilayer Film on Aluminum and Its Corrosion Resistance Properties. *Langmuir* **2009**, *25*, 9894–9897. [CrossRef]
36. Scarpellini, D.; Falconi, C.; Gaudio, P.; Mattoccia, A.; Medaglia, P.G.; Orsini, A.; Pizzoferrato, R.; Richetta, M. Morphology of Zn/Al layered double hydroxide nanosheets grown onto aluminum thin films. *Microelectron. Eng.* **2014**, *126*, 129–133. [CrossRef]
37. Prestopino, G.; Arrabito, G.; Generosi, A.; Mattoccia, A.; Paci, B.; Perez, G.; Verona-Rinati, G.; Medaglia, P.G. Emerging switchable ultraviolet photoluminescence in dehydrated Zn/Al layered double hydroxide nanoplatelets. *Sci. Rep.* **2019**, *9*, 11498. [CrossRef]
38. Forticaux, A.; Dang, L.; Liang, H.; Jin, S. Controlled Synthesis of Layered Double Hydroxide Nanoplates Driven by Screw Dislocations. *Nano Lett.* **2015**, *15*, 3403–3409. [CrossRef]
39. Liu, J.; Li, Y.; Huang, X.; Li, G.; Li, Z. Layered Double Hydroxide Nano- and Microstructures Grown Directly on Metal Substrates and Their Calcined Products for Application as Li-Ion Battery Electrodes. *Adv. Funct. Mater.* **2008**, *18*, 1448–1458. [CrossRef]
40. Miyata, S. Anion-Exchange Properties of Hydrotalcite-Like Compounds. *Clays Clay Miner.* **1983**, *31*, 305–311. [CrossRef]
41. Meyn, M.; Beneke, K.; Lagaly, G. Anion-exchange reactions of layered double hydroxides. *Inorg. Chem.* **1990**, *29*, 5201–5207. [CrossRef]
42. Radha, A.V.; Vishnu Kamath, P.; Shivakumara, C. Mechanism of the anion exchange reactions of the layered double hydroxides (LDHs) of Ca and Mg with Al. *Solid State Sci.* **2005**, *7*, 1180–1187. [CrossRef]
43. Prasanna, S.V.; Kamath, P.V. Anion-Exchange Reactions of Layered Double Hydroxides: Interplay between Coulombic and H-Bonding Interactions. *Ind. Eng. Chem. Res.* **2009**, *48*, 6315–6320. [CrossRef]
44. Tavares, S.R.; Haddad, J.F.S.; Ivo, R.; Moraes, P.; Leitão, A.A. Computational exploration of the anion exchange on the basal surface of layered double hydroxides by molecular dynamics. *Appl. Surf. Sci.* **2020**, *513*, 145743. [CrossRef]
45. Debecker, D.P.; Gaigneaux, E.M.; Busca, G. Exploring, Tuning, and Exploiting the Basicity of Hydrotalcites for Applications in Heterogeneous Catalysis. *Chem. Eur. J.* **2009**, *15*, 3920–3935. [CrossRef] [PubMed]
46. Manohara, G.V.; Prasanna, S.V.; Kamath, P.V. Structure and Composition of the Layered Double Hydroxides of Mg and Fe: Implications for Anion-Exchange Reactions. *Eur. J. Inorg. Chem.* **2011**, *2011*, 2624–2630. [CrossRef]
47. Xu, M.; Wei, M. Layered Double Hydroxide-Based Catalysts: Recent Advances in Preparation, Structure, and Applications. *Adv. Funct. Mater.* **2018**, *28*, 1802943. [CrossRef]
48. Sideris, P.J.; Nielsen, U.G.; Gan, Z.; Grey, C.P. Mg/Al Ordering in Layered Double Hydroxides Revealed by Multinuclear NMR Spectroscopy. *Science* **2008**, *321*, 113–117. [CrossRef]
49. Vucelic, M. Cation Ordering in Synthetic Layered Double Hydroxides. *Clays Clay Miner.* **1997**, *45*, 803–813. [CrossRef]
50. Kim, D.; Huang, C.; Lee, H.; Han, I.; Kang, S.; Kwon, S.; Lee, J.; Han, Y.; Kim, H. Hydrotalcite-type catalysts for narrow-range oxyethylation of 1-dodecanol using ethyleneoxide. *Appl. Catal. A Gen.* **2003**, *249*, 229–240. [CrossRef]
51. Krivovichev, S.V.; Yakovenchuk, V.N.; Zhitova, E.S. Natural Double Layered Hydroxides: Structure, Chemistry, and Information Storage Capacity. In *Minerals as Advanced Materials II*; Krivovichev, S.V., Ed.; Springer Berlin Heidelberg: Berlin/Heidelberg, Germany, 2011; pp. 87–102, ISBN 978-3-642-20017-5.
52. Kuma, K.; Paplawsky, W.; Gedulin, B.; Arrhenius, G. Mixed-valence hydroxides as bioorganic host minerals. *Orig. Life Evol. Biosph.* **1989**, *19*, 573–601. [CrossRef]
53. Arrhenius, G.O. Crystals and Life. *HCA* **2003**, *86*, 1569–1586. [CrossRef]
54. Erastova, V.; Degiacomi, M.T.; Fraser, D.G.; Greenwell, H.C. Mineral surface chemistry control for origin of prebiotic peptides. *Nat. Commun.* **2017**, *8*, 2033. [CrossRef]
55. Greenwell, H.C.; Coveney, P.V. Layered Double Hydroxide Minerals as Possible Prebiotic Information Storage and Transfer Compounds. *Orig. Life Evol. Biosph.* **2006**, *36*, 13–37. [CrossRef]
56. Sanchez, C.; Arribart, H.; Giraud Guille, M.M. Biomimetism and bioinspiration as tools for the design of innovative materials and systems. *Nat. Mater.* **2005**, *4*, 277–288. [CrossRef] [PubMed]
57. Ruiz-Hitzky, E.; Darder, M.; Aranda, P.; Ariga, K. Advances in Biomimetic and Nanostructured Biohybrid Materials. *Adv. Mater.* **2010**, *22*, 323–336. [CrossRef] [PubMed]

58. Chen, P.-Y.; McKittrick, J.; Meyers, M.A. Biological materials: Functional adaptations and bioinspired designs. *Prog. Mater. Sci.* **2012**, *57*, 1492–1704. [CrossRef]
59. Zhang, C.; Mcadams, D.A.; Grunlan, J.C. Nano/Micro-Manufacturing of Bioinspired Materials: A Review of Methods to Mimic Natural Structures. *Adv. Mater.* **2016**, *28*, 6292–6321. [CrossRef]
60. Gong, C.; Sun, S.; Zhang, Y.; Sun, L.; Su, Z.; Wu, A.; Wei, G. Hierarchical nanomaterials *via* biomolecular self-assembly and bioinspiration for energy and environmental applications. *Nanoscale* **2019**, *11*, 4147–4182. [CrossRef]
61. Vijayan, P.P.; Puglia, D. Biomimetic multifunctional materials: A review. *Emergent Mater.* **2019**, *2*, 391–415. [CrossRef]
62. Ruiz-Hitzky, E.; Darder, M.; Wicklein, B.; Castro-Smirnov, F.A.; Aranda, P. Clay-based biohybrid materials for biomedical and pharmaceutical applications. *Clays Clay Miner.* **2019**, *67*, 44–58. [CrossRef]
63. Xu, S.; Zhao, J.; Yu, Q.; Qiu, X.; Sasaki, K. Effect of Natural Organic Matter Model Compounds on the Structure Memory Effect of Different Layered Double Hydroxides. *ACS Earth Space Chem.* **2019**, *3*, 2175–2189. [CrossRef]
64. Lambert, J.-F. Origins of life: From the mineral to the biochemical world. *BIO Web Conf.* **2015**, *4*, 00012. [CrossRef]
65. Orgel, L.E. The origin of life—A review of facts and speculations. *Trends Biochem. Sci.* **1998**, *23*, 491–495. [CrossRef]
66. Ferus, M.; Pietrucci, F.; Saitta, A.M.; Knížek, A.; Kubelík, P.; Ivanek, O.; Shestivska, V.; Civiš, S. Formation of nucleobases in a Miller–Urey reducing atmosphere. *Proc. Natl. Acad. Sci. USA* **2017**, *114*, 4306–4311. [CrossRef]
67. Clark, B.; Kolb, V. Comet Pond II: Synergistic Intersection of Concentrated Extraterrestrial Materials and Planetary Environments to Form Procreative Darwinian Ponds. *Life* **2018**, *8*, 12. [CrossRef]
68. Martin, W.; Russell, M.J. On the origins of cells: A hypothesis for the evolutionary transitions from abiotic geochemistry to chemoautotrophic prokaryotes, and from prokaryotes to nucleated cells. *Phil. Trans. R. Soc. Lond. B* **2003**, *358*, 59–85. [CrossRef]
69. Das, T.; Ghule, S.; Vanka, K. Insights Into the Origin of Life: Did It Begin from HCN and $H_2O$? *ACS Cent. Sci.* **2019**, *5*, 1532–1540. [CrossRef]
70. Meisner, J.; Zhu, X.; Martínez, T.J. Computational Discovery of the Origins of Life. *ACS Cent. Sci.* **2019**, *5*, 1493–1495. [CrossRef]
71. Rimola, A.; Sodupe, M.; Ugliengo, P. Role of Mineral Surfaces in Prebiotic Chemical Evolution. In Silico Quantum Mechanical Studies. *Life* **2019**, *9*, 10. [CrossRef]
72. Ponce, A. Radionuclide-induced defect sites in iron-bearing minerals may have accelerated the emergence of life. *Interface Focus* **2019**, *9*, 20190085. [CrossRef]
73. Sojo, V.; Herschy, B.; Whicher, A.; Camprubí, E.; Lane, N. The Origin of Life in Alkaline Hydrothermal Vents. *Astrobiology* **2016**, *16*, 181–197. [CrossRef]
74. Martin, W.; Baross, J.; Kelley, D.; Russell, M.J. Hydrothermal vents and the origin of life. *Nat. Rev. Microbiol.* **2008**, *6*, 805–814. [CrossRef]
75. Braterman, P.S.; Cairns-Smith, A.G. Photoprecipitation and the banded iron-formations—Some quantitative aspects. *Orig. Life Evol. Biosph.* **1987**, *17*, 221–228. [CrossRef]
76. Russell, M.J. Green rust: The simple organizing 'seed' of all life? *Life* **2018**, *8*. [CrossRef] [PubMed]
77. Bernal, J.D. The Physical Basis of Life. *Proc. Phys. Soc. Sect. A* **1949**, *62*, 537–558. [CrossRef]
78. Cairns-Smith, A.G. *Genetic Takeover and the Mineral Origins of Life*, 1st ed.; Cambridge Univ. Press: Cambridge, UK, 1987; ISBN 978-0-521-34682-5.
79. Ferris, J.P. Montmorillonite Catalysis of 30–50 Mer Oligonucleotides: Laboratory Demonstration of Potential Steps in the Origin of the RNA World. *Orig. Life Evol. Biosph.* **2002**, *32*, 311–332. [CrossRef] [PubMed]
80. Lahav, N.; White, D.; Chang, S. Peptide formation in the prebiotic era: Thermal condensation of glycine in fluctuating clay environments. *Science* **1978**, *201*, 67–69. [CrossRef]
81. Hanczyc, M.M.; Fujikawa, S.M.; Szostak, J.W. Experimental Models of Primitive Cellular Compartments: Encapsulation, Growth, and Division. *Science* **2003**, *302*, 618–622. [CrossRef]
82. Swadling, J.B.; Coveney, P.V.; Christopher Greenwell, H. Stability of free and mineral-protected nucleic acids: Implications for the RNA world. *Geochim. Cosmochim. Acta* **2012**, *83*, 360–378. [CrossRef]

83. Grégoire, B.; Greenwell, H.C.; Fraser, D.G. Peptide Formation on Layered Mineral Surfaces: The Key Role of Brucite-like Minerals on the Enhanced Formation of Alanine Dipeptides. *ACS Earth Space Chem.* **2018**, *2*, 852–862. [CrossRef]
84. Vasti, C.; Ambroggio, E.; Rojas, R.; Giacomelli, C.E. A closer look into the physical interactions between lipid membranes and layered double hydroxide nanoparticles. *Colloids Surf. B Biointerfaces* **2020**, *191*, 110998. [CrossRef]
85. Bernhardt, H. Making Molecules with Clay: Layered Double Hydroxides, Pentopyranose Nucleic Acids and the Origin of Life. *Life* **2019**, *9*, 19. [CrossRef]
86. Suen, N.-T.; Hung, S.-F.; Quan, Q.; Zhang, N.; Xu, Y.-J.; Chen, H.M. Electrocatalysis for the oxygen evolution reaction: Recent development and future perspectives. *Chem. Soc. Rev.* **2017**, *46*, 337–365. [CrossRef]
87. Lu, X.; Xue, H.; Gong, H.; Bai, M.; Tang, D.; Ma, R.; Sasaki, T. 2D Layered Double Hydroxide Nanosheets and Their Derivatives Toward Efficient Oxygen Evolution Reaction. *Nano-Micro Lett.* **2020**, *12*, 86. [CrossRef]
88. Wang, L.; Arrabito, G. Hybrid, multiplexed, functional DNA nanotechnology for bioanalysis. *Analyst* **2015**, *140*, 5821–5848. [CrossRef]
89. Yadav, M.; Kumar, R.; Krishnamurthy, R. Chemistry of Abiotic Nucleotide Synthesis. *Chem. Rev.* **2020**, *120*, 4766–4805. [CrossRef]
90. Baú, J.P.T.; Villafañe-Barajas, S.A.; da Costa, A.C.S.; Negrón-Mendoza, A.; Colín-Garcia, M.; Zaia, D.A.M. Adenine Adsorbed onto Montmorillonite Exposed to Ionizing Radiation: Essays on Prebiotic Chemistry. *Astrobiology* **2020**, *20*, 26–38. [CrossRef] [PubMed]
91. Li, Y.; Yan, Z.; Xiao, J.; Yue, T. DNA-conjugated layered double hydroxides penetrating into a plasma membrane: Layer size, thickness and DNA grafting density matter. *NanoImpact* **2020**, *18*, 100222. [CrossRef]
92. Murase, N.; Gonda, K. Adsorption of Liposomes by Clay. *J. Biochem.* **1982**, *92*, 271–273. [CrossRef]
93. Konnova, S.A.; Sharipova, I.R.; Demina, T.A.; Osin, Y.N.; Yarullina, D.R.; Ilinskaya, O.N.; Lvov, Y.M.; Fakhrullin, R.F. Biomimetic cell-mediated three-dimensional assembly of halloysite nanotubes. *Chem. Commun.* **2013**, *49*, 4208–4210. [CrossRef]
94. Itoh, T.; Ohta, N.; Shichi, T.; Yui, T.; Takagi, K. The Self-Assembling Properties of Stearate Ions in Hydrotalcite Clay Composites. *Langmuir* **2003**, *19*, 9120–9126. [CrossRef]
95. Aisawa, S.; Kudo, H.; Hoshi, T.; Takahashi, S.; Hirahara, H.; Umetsu, Y.; Narita, E. Intercalation behavior of amino acids into Zn–Al-layered double hydroxide by calcination–rehydration reaction. *J. Solid State Chem.* **2004**, *177*, 3987–3994. [CrossRef]
96. Wang, J.; Zhang, W.; Hao, L.; Sun, J.; Zhang, W.; Guo, C.; Mu, Y.; Ji, W.; Yu, C.; Yuan, F. Amino acid–intercalated layered double hydroxide core @ ordered porous silica shell as drug carriers: Design and applications. *J. Mater. Res.* **2019**, *34*, 3747–3756. [CrossRef]
97. Paecht-Horowitz, M. The possible role of clays in prebiotic peptide synthesis. *Orig. Life* **1974**, *5*, 173–187. [CrossRef]
98. Yadollahi, M.; Namazi, H.; Barkhordari, S. Preparation and properties of carboxymethyl cellulose/layered double hydroxide bionanocomposite films. *Carbohydr. Polym.* **2014**, *108*, 83–90. [CrossRef] [PubMed]
99. Zhang, L.; Chen, K.; He, L. Super-reinforced photothermal stability of cellulose nanofibrils films by armour-type ordered doping Mg-Al layered double hydroxides. *Carbohydr. Polym.* **2019**, *212*, 229–234. [CrossRef]
100. Liang, B.; Wang, J.; Shu, Y.; Yin, P.; Guo, L. A biomimetic ion-crosslinked layered double hydroxide/alginate hybrid film. *RSC Adv.* **2017**, *7*, 32601–32606. [CrossRef]
101. Ai, Y.; Xie, R.; Xiong, J.; Liang, Q. Microfluidics for Biosynthesizing: From Droplets and Vesicles to Artificial Cells. *Small* **2020**, *16*, 1903940. [CrossRef]
102. Ma, Q.; Song, Y.; Sun, W.; Cao, J.; Yuan, H.; Wang, X.; Sun, Y.; Shum, H.C. Cell-Inspired All-Aqueous Microfluidics: From Intracellular Liquid–Liquid Phase Separation toward Advanced Biomaterials. *Adv. Sci.* **2020**, *7*, 1903359. [CrossRef] [PubMed]
103. Arrabito, G.; Reisewitz, S.; Dehmelt, L.; Bastiaens, P.I.; Pignataro, B.; Schroeder, H.; Niemeyer, C.M. Biochips for Cell Biology by Combined Dip-Pen Nanolithography and DNA-Directed Protein Immobilization. *Small* **2013**, *9*, 4243–4249. [CrossRef] [PubMed]
104. Arrabito, G.; Schroeder, H.; Schröder, K.; Filips, C.; Marggraf, U.; Dopp, C.; Venkatachalapathy, M.; Dehmelt, L.; Bastiaens, P.I.H.; Neyer, A.; et al. Configurable Low-Cost Plotter Device for Fabrication of Multi-Color Sub-Cellular Scale Microarrays. *Small* **2014**, *10*, 2870–2876. [CrossRef] [PubMed]

105. Bracha, D.; Karzbrun, E.; Daube, S.S.; Bar-Ziv, R.H. Emergent Properties of Dense DNA Phases toward Artificial Biosystems on a Surface. *Acc. Chem. Res.* **2014**, *47*, 1912–1921. [CrossRef]
106. Arrabito, G.; Cavaleri, F.; Montalbano, V.; Vetri, V.; Leone, M.; Pignataro, B. Monitoring few molecular binding events in scalable confined aqueous compartments by raster image correlation spectroscopy (CADRICS). *Lab Chip* **2016**, *16*, 4666–4676. [CrossRef]
107. Arrabito, G.; Cavaleri, F.; Porchetta, A.; Ricci, F.; Vetri, V.; Leone, M.; Pignataro, B. Printing Life-Inspired Subcellular Scale Compartments with Autonomous Molecularly Crowded Confinement. *Adv. Biosyst.* **2019**, *3*, 1900023. [CrossRef] [PubMed]
108. Cui, Y.; van Duijneveldt, J.S. Microcapsules Composed of Cross-Linked Organoclay. *Langmuir* **2012**, *28*, 1753–1757. [CrossRef]
109. Subramaniam, A.B.; Wan, J.; Gopinath, A.; Stone, H.A. Semi-permeable vesicles composed of natural clay. *Soft Matter* **2011**, *7*, 2600. [CrossRef]
110. Li, M.; Harbron, R.L.; Weaver, J.V.M.; Binks, B.P.; Mann, S. Electrostatically gated membrane permeability in inorganic protocells. *Nat. Chem.* **2013**, *5*, 529–536. [CrossRef] [PubMed]
111. Kumar, B.V.V.S.P.; Patil, A.J.; Mann, S. Enzyme-powered motility in buoyant organoclay/DNA protocells. *Nat. Chem.* **2018**, *10*, 1154–1163. [CrossRef] [PubMed]
112. Arrabito, G.; Pignataro, B. Solution Processed Micro- and Nano-Bioarrays for Multiplexed Biosensing. *Anal. Chem.* **2012**, *84*, 5450–5462. [CrossRef] [PubMed]
113. Choi, H.W.; Zhou, T.; Singh, M.; Jabbour, G.E. Recent developments and directions in printed nanomaterials. *Nanoscale* **2015**, *7*, 3338–3355. [CrossRef]
114. Miccichè, C.; Arrabito, G.; Amato, F.; Buscarino, G.; Agnello, S.; Pignataro, B. Inkjet printing Ag nanoparticles for SERS hot spots. *Anal. Methods* **2018**, *10*, 3215–3223. [CrossRef]
115. Arrabito, G.; Errico, V.; De Ninno, A.; Cavaleri, F.; Ferrara, V.; Pignataro, B.; Caselli, F. Oil-in-Water fL Droplets by Interfacial Spontaneous Fragmentation and Their Electrical Characterization. *Langmuir* **2019**, *35*, 4936–4945. [CrossRef]
116. Zhang, Y.; Evans, J.R.G. Morphologies developed by the drying of droplets containing dispersed and aggregated layered double hydroxide platelets. *J. Colloid Interface Sci.* **2013**, *395*, 11–17. [CrossRef]
117. Zhang, Y.; Evans, J.R.G. Alignment of layered double hydroxide platelets. *Colloids Surfaces A Physicochem. Eng. Asp.* **2012**, *408*, 71–78. [CrossRef]
118. Zheng, Y.-M.; Li, N.; Zhang, W.-D. Preparation of nanostructured microspheres of Zn–Mg–Al layered double hydroxides with high adsorption property. *Colloids Surfaces A Physicochem. Eng. Asp.* **2012**, *415*, 195–201. [CrossRef]
119. Chen, Y.; Jing, C.; Zhang, X.; Jiang, D.; Liu, X.; Dong, B.; Feng, L.; Li, S.; Zhang, Y. Acid-salt treated CoAl layered double hydroxide nanosheets with enhanced adsorption capacity of methyl orange dye. *J. Colloid Interface Sci.* **2019**, *548*, 100–109. [CrossRef] [PubMed]
120. Sun, J.; Bao, B.; He, M.; Zhou, H.; Song, Y. Recent Advances in Controlling the Depositing Morphologies of Inkjet Droplets. *ACS Appl. Mater. Interfaces* **2015**, *7*, 28086–28099. [CrossRef]
121. Zhu, H.; Huang, S.; Yang, Z.; Liu, T. Oriented printable layered double hydroxide thin films via facile filtration. *J. Mater. Chem.* **2011**, *21*, 2950. [CrossRef]
122. Vijayamma, R.; Kalarikkal, N.; Thomas, S. Layered double hydroxide based nanocomposites for biomedical applications. In *Layered Double Hydroxide Polymer Nanocomposites*; Elsevier: Amsterdam, The Netherlands, 2020; pp. 677–714, ISBN 978-0-08-102261-0.
123. Chatterjee, A.; Bharadiya, P.; Hansora, D. Layered double hydroxide based bionanocomposites. *Appl. Clay Sci.* **2019**, *177*, 19–36. [CrossRef]
124. Shu, Y.; Yin, P.; Wang, J.; Liang, B.; Wang, H.; Guo, L. Bioinspired Nacre-like Heparin/Layered Double Hydroxide Film with Superior Mechanical, Fire-Shielding, and UV-Blocking Properties. *Ind. Eng. Chem. Res.* **2014**, *53*, 3820–3826. [CrossRef]
125. Shu, Y.; Yin, P.; Liang, B.; Wang, H.; Guo, L. Bioinspired Design and Assembly of Layered Double Hydroxide/Poly(vinyl alcohol) Film with High Mechanical Performance. *ACS Appl. Mater. Interfaces* **2014**, *6*, 15154–15161. [CrossRef]
126. Meng, Y.; Zhang, B.; Su, J.; Han, J. Bioinspired Design of LDH-Based Mobile Building Materials with Enhanced Mechanical and Ultraviolet-Shielding Performance. *Macromol. Mater. Eng.* **2019**, *304*, 1900276. [CrossRef]

127. Liu, P.; Zhang, Y.; Liu, S.; Zhang, Y.; Du, Z.; Qu, L. Bio-inspired fabrication of fire-retarding, magnetic-responsive, superhydrophobic sponges for oil and organics collection. *Appl. Clay Sci.* **2019**, *172*, 19–27. [CrossRef]
128. Wang, Z.; Shen, X.; Qian, T.; Xu, K.; Sun, Q.; Jin, C. Fabrication of Superhydrophobic Mg/Al Layered Double Hydroxide (LDH) Coatings on Medium Density Fiberboards (MDFs) with Flame Retardancy. *Materials* **2018**, *11*, 1113. [CrossRef] [PubMed]
129. Wu, H.; Shi, Z.; Zhang, X.; Qasim, A.M.; Xiao, S.; Zhang, F.; Wu, Z.; Wu, G.; Ding, K.; Chu, P.K. Achieving an acid resistant surface on magnesium alloy via bio-inspired design. *Appl. Surf. Sci.* **2019**, *478*, 150–161. [CrossRef]
130. Yu, J.; Buffet, J.-C.; O'Hare, D. Aspect Ratio Control of Layered Double Hydroxide Nanosheets and Their Application for High Oxygen Barrier Coating in Flexible Food Packaging. *ACS Appl. Mater. Interfaces* **2020**, *12*, 10973–10982. [CrossRef]
131. Cui, P.; Wang, J.; Xiong, J.; Li, S.; Zhang, W.; Liu, X.; Gu, G.; Guo, J.; Zhang, B.; Cheng, G.; et al. Meter-scale fabrication of water-driven triboelectric nanogenerator based on in-situ grown layered double hydroxides through a bottom-up approach. *Nano Energy* **2020**, *71*, 104646. [CrossRef]
132. Sun, J.; Li, P.; Qu, J.; Lu, X.; Xie, Y.; Gao, F.; Li, Y.; Gang, M.; Feng, Q.; Liang, H.; et al. Electricity generation from a Ni-Al layered double hydroxide-based flexible generator driven by natural water evaporation. *Nano Energy* **2019**, *57*, 269–278. [CrossRef]
133. Tian, J.; Zang, Y.; Sun, J.; Qu, J.; Gao, F.; Liang, G. Surface charge density-dependent performance of Ni–Al layered double hydroxide-based flexible self-powered generators driven by natural water evaporation. *Nano Energy* **2020**, *70*, 104502. [CrossRef]
134. Xu, S.; Dall'Agnese, Y.; Wei, G.; Zhang, C.; Gogotsi, Y.; Han, W. Screen-printable microscale hybrid device based on MXene and layered double hydroxide electrodes for powering force sensors. *Nano Energy* **2018**, *50*, 479–488. [CrossRef]
135. Guo, Y.; Zhang, S.; Wang, J.; Liu, Z.; Liu, Y. Facile preparation of high-performance cobalt–manganese layered double hydroxide/polypyrrole composite for battery-type asymmetric supercapacitors. *J. Alloys Compd.* **2020**, *832*, 154899. [CrossRef]
136. Ren, Y.; Feng, J. Skin-Inspired Multifunctional Luminescent Hydrogel Containing Layered Rare-Earth Hydroxide with 3D Printability for Human Motion Sensing. *ACS Appl. Mater. Interfaces* **2020**, *12*, 6797–6805. [CrossRef]
137. Beigi, F.; Mousavi, M.S.S.; Manteghi, F.; Kolahdouz, M. Doped nafion-layered double hydroxide nanoparticles as a modified ionic polymer metal composite sheet for a high-responsive humidity sensor. *Appl. Clay Sci.* **2018**, *166*, 131–136. [CrossRef]
138. Grätzel, M. Photoelectrochemical cells. *Nature* **2001**, *414*, 338–344. [CrossRef] [PubMed]
139. Gray, H.B. Powering the planet with solar fuel. *Nat. Chem.* **2009**, *1*, 7. [CrossRef] [PubMed]
140. Zhang, M.; de Respinis, M.; Frei, H. Time-resolved observations of water oxidation intermediates on a cobalt oxide nanoparticle catalyst. *Nat. Chem.* **2014**, *6*, 362–367. [CrossRef] [PubMed]
141. Liu, Y.; Li, Q.; Si, R.; Li, G.-D.; Li, W.; Liu, D.-P.; Wang, D.; Sun, L.; Zhang, Y.; Zou, X. Coupling Sub-Nanometric Copper Clusters with Quasi-Amorphous Cobalt Sulfide Yields Efficient and Robust Electrocatalysts for Water Splitting Reaction. *Adv. Mater.* **2017**, *29*, 1606200. [CrossRef] [PubMed]
142. Wang, Y.; Jiang, K.; Zhang, H.; Zhou, T.; Wang, J.; Wei, W.; Yang, Z.; Sun, X.; Cai, W.-B.; Zheng, G. Bio-Inspired Leaf-Mimicking Nanosheet/Nanotube Heterostructure as a Highly Efficient Oxygen Evolution Catalyst. *Adv. Sci.* **2015**, *2*, 1500003. [CrossRef] [PubMed]
143. Wei, W.; He, W.; Shi, B.; Dong, G.; Lu, X.; Zeng, M.; Gao, X.; Wang, Q.; Zhou, G.; Liu, J.-M.; et al. A bio-inspired 3D quasi-fractal nanostructure for an improved oxygen evolution reaction. *Chem. Commun.* **2019**, *55*, 357–360. [CrossRef] [PubMed]
144. Trogadas, P.; Coppens, M.-O. Nature-inspired electrocatalysts and devices for energy conversion. *Chem. Soc. Rev.* **2020**. [CrossRef]
145. Xu, S.-M.; Pan, T.; Dou, Y.-B.; Yan, H.; Zhang, S.-T.; Ning, F.-Y.; Shi, W.-Y.; Wei, M. Theoretical and Experimental Study on $M^{II}$ $M^{III}$ -Layered Double Hydroxides as Efficient Photocatalysts toward Oxygen Evolution from Water. *J. Phys. Chem. C* **2015**, *119*, 18823–18834. [CrossRef]
146. Dionigi, F.; Strasser, P. NiFe-Based (Oxy)hydroxide Catalysts for Oxygen Evolution Reaction in Non-Acidic Electrolytes. *Adv. Energy Mater.* **2016**, *6*, 1600621. [CrossRef]

147. Sun, H.; Yan, Z.; Liu, F.; Xu, W.; Cheng, F.; Chen, J. Self-Supported Transition-Metal-Based Electrocatalysts for Hydrogen and Oxygen Evolution. *Adv. Mater.* **2020**, *32*, 1806326. [CrossRef]
148. Lu, Z.; Xu, W.; Zhu, W.; Yang, Q.; Lei, X.; Liu, J.; Li, Y.; Sun, X.; Duan, X. Three-dimensional NiFe layered double hydroxide film for high-efficiency oxygen evolution reaction. *Chem. Commun.* **2014**, *50*, 6479–6482. [CrossRef] [PubMed]
149. Song, F.; Hu, X. Exfoliation of layered double hydroxides for enhanced oxygen evolution catalysis. *Nat. Commun.* **2014**, *5*, 4477. [CrossRef] [PubMed]
150. Liang, H.; Meng, F.; Cabán-Acevedo, M.; Li, L.; Forticaux, A.; Xiu, L.; Wang, Z.; Jin, S. Hydrothermal Continuous Flow Synthesis and Exfoliation of NiCo Layered Double Hydroxide Nanosheets for Enhanced Oxygen Evolution Catalysis. *Nano Lett.* **2015**, *15*, 1421–1427. [CrossRef] [PubMed]
151. Wang, Y.; Zhang, Y.; Liu, Z.; Xie, C.; Feng, S.; Liu, D.; Shao, M.; Wang, S. Layered Double Hydroxide Nanosheets with Multiple Vacancies Obtained by Dry Exfoliation as Highly Efficient Oxygen Evolution Electrocatalysts. *Angew. Chem. Int. Ed.* **2017**, *56*, 5867–5871. [CrossRef] [PubMed]
152. Wang, Y.; Xie, C.; Zhang, Z.; Liu, D.; Chen, R.; Wang, S. In Situ Exfoliated, N-Doped, and Edge-Rich Ultrathin Layered Double Hydroxides Nanosheets for Oxygen Evolution Reaction. *Adv. Funct. Mater.* **2018**, *28*, 1703363. [CrossRef]
153. Gong, M.; Li, Y.; Wang, H.; Liang, Y.; Wu, J.Z.; Zhou, J.; Wang, J.; Regier, T.; Wei, F.; Dai, H. An Advanced Ni–Fe Layered Double Hydroxide Electrocatalyst for Water Oxidation. *J. Am. Chem. Soc.* **2013**, *135*, 8452–8455. [CrossRef]
154. Long, X.; Li, J.; Xiao, S.; Yan, K.; Wang, Z.; Chen, H.; Yang, S. A Strongly Coupled Graphene and FeNi Double Hydroxide Hybrid as an Excellent Electrocatalyst for the Oxygen Evolution Reaction. *Angew. Chem. Int. Ed.* **2014**, *53*, 7584–7588. [CrossRef]
155. Ma, W.; Ma, R.; Wang, C.; Liang, J.; Liu, X.; Zhou, K.; Sasaki, T. A Superlattice of Alternately Stacked Ni–Fe Hydroxide Nanosheets and Graphene for Efficient Splitting of Water. *ACS Nano* **2015**, *9*, 1977–1984. [CrossRef]
156. Zhang, X.; Marianov, A.N.; Jiang, Y.; Cazorla, C.; Chu, D. Hierarchically Constructed Silver Nanowire@Nickel–Iron Layered Double Hydroxide Nanostructures for Electrocatalytic Water Splitting. *ACS Appl. Nano Mater.* **2020**, *3*, 887–895. [CrossRef]
157. Chen, B.; Zhang, Z.; Kim, S.; Baek, M.; Kim, D.; Yong, K. A biomimetic nanoleaf electrocatalyst for robust oxygen evolution reaction. *Appl. Catal. B Environ.* **2019**, *259*, 118017. [CrossRef]
158. Yang, W.; Li, J.; Liu, M.; Ng, D.H.L.; Liu, Y.; Sun, X.; Yang, J. Bioinspired hierarchical CoAl-LDH/MFe2O4(Ni, Zn, Co) as peroxidase mimics for colorimetric detection of glucose. *Appl. Clay Sci.* **2019**, *181*, 105238. [CrossRef]
159. Yang, W.; Li, J.; Yang, J.; Liu, Y.; Xu, Z.; Sun, X.; Wang, F.; Ng, D.H.L. Biomass-derived hierarchically porous CoFe-LDH/CeO2hybrid with peroxidase-like activity for colorimetric sensing of H2O2 and glucose. *J. Alloys Compd.* **2020**, *815*, 152276. [CrossRef]
160. Yang, W.; Li, J.; Wang, M.; Sun, X.; Liu, Y.; Yang, J.; Ng, D.H.L. A colorimetric strategy for ascorbic acid sensing based on the peroxidase-like activity of core-shell Fe3O4/CoFe-LDH hybrid. *Colloids Surf. B Biointerfaces* **2020**, *188*, 110742. [CrossRef] [PubMed]
161. Zhang, Y.; Tian, J.; Liu, S.; Wang, L.; Qin, X.; Lu, W.; Chang, G.; Luo, Y.; Asiri, A.M.; Al-Youbi, A.O.; et al. Novel application of CoFe layered double hydroxide nanoplates for colorimetric detection of H2O2 and glucose. *Analyst* **2012**, *137*, 1325. [CrossRef]
162. Su, L.; Yu, X.; Qin, W.; Dong, W.; Wu, C.; Zhang, Y.; Mao, G.; Feng, S. One-step analysis of glucose and acetylcholine in water based on the intrinsic peroxidase-like activity of Ni/Co LDHs microspheres. *J. Mater. Chem. B* **2017**, *5*, 116–122. [CrossRef]
163. Zhan, T.; Kang, J.; Li, X.; Pan, L.; Li, G.; Hou, W. NiFe layered double hydroxide nanosheets as an efficiently mimic enzyme for colorimetric determination of glucose and H2O2. *Sensors Actuators B Chem.* **2018**, *255*, 2635–2642. [CrossRef]
164. Fazli, G.; Esmaeilzadeh Bahabadi, S.; Adlnasab, L.; Ahmar, H. A glassy carbon electrode modified with a nanocomposite prepared from Pd/Al layered double hydroxide and carboxymethyl cellulose for voltammetric sensing of hydrogen peroxide. *Microchim. Acta* **2019**, *186*, 821. [CrossRef] [PubMed]

165. Wang, L.; Chen, X.; Liu, C.; Yang, W. Non-enzymatic acetylcholine electrochemical biosensor based on flower-like NiAl layered double hydroxides decorated with carbon dots. *Sensors Actuators B Chem.* **2016**, *233*, 199–205. [CrossRef]
166. Zhao, Y.; Chen, G.; Bian, T.; Zhou, C.; Waterhouse, G.I.N.; Wu, L.-Z.; Tung, C.-H.; Smith, L.J.; O'Hare, D.; Zhang, T. Defect-Rich Ultrathin ZnAl-Layered Double Hydroxide Nanosheets for Efficient Photoreduction of $CO_2$ to CO with Water. *Adv. Mater.* **2015**, *27*, 7824–7831. [CrossRef]
167. Liu, P.F.; Yang, S.; Zhang, B.; Yang, H.G. Defect-Rich Ultrathin Cobalt–Iron Layered Double Hydroxide for Electrochemical Overall Water Splitting. *ACS Appl. Mater. Interfaces* **2016**, *8*, 34474–34481. [CrossRef]
168. Nie, Q.; Ma, J.; Xie, Y. A new synthesis method of ultrathin Zn-Al layered double hydroxide with super adsorption capacity. *IOP Conf. Ser. Earth Environ. Sci.* **2019**, *300*, 052003. [CrossRef]
169. Zhao, G.; Zou, J.; Chen, X.; Yu, J.; Jiao, F. Layered double hydroxides materials for photo(electro-) catalytic applications. *Chem. Eng. J.* **2020**, *397*, 125407. [CrossRef]
170. Zhu, L.; Li, H.; Yin, Y.; Cui, Z.; Ma, C.; Li, X.; Xue, Q. One-step synthesis of a robust and anti-oil-fouling biomimetic cactus-like hierarchical architecture for highly efficient oil/water separation. *Environ. Sci. Nano* **2020**, *7*, 903–911. [CrossRef]
171. Abolghasemi, M.M.; Amirifard, H.; Piryaei, M. Bio template route for fabrication of a hybrid material composed of hierarchical boehmite, layered double hydroxides (Mg-Al) and porous carbon on a steel fiber for solid phase microextraction of agrochemicals. *Microchim. Acta* **2019**, *186*, 678. [CrossRef] [PubMed]
172. Sriram, G.; Uthappa, U.T.; Losic, D.; Kigga, M.; Jung, H.-Y.; Kurkuri, M.D. Mg–Al-Layered Double Hydroxide (LDH) Modified Diatoms for Highly Efficient Removal of Congo Red from Aqueous Solution. *Appl. Sci.* **2020**, *10*, 2285. [CrossRef]
173. Sun, Q.; Tang, M.; Hendriksen, P.V.; Chen, B. Biotemplated fabrication of a 3D hierarchical structure of magnetic ZnFe2O4/MgAl-LDH for efficient elimination of dye from water. *J. Alloys Compd.* **2020**, *829*, 154552. [CrossRef]
174. Bing, X.; Li, J.; Liu, J.; Cui, X.; Ji, F. Biomimetic synthesis of Bi2O3/Bi2WO6/MgAl-CLDH hybrids from lotus pollen and their enhanced adsorption and photocatalysis performance. *J. Photochem. Photobiol. A Chem.* **2018**, *364*, 449–460. [CrossRef]
175. Baruah, A.; Mondal, S.; Sahoo, L.; Gautam, U.K. Ni-Fe-layered double hydroxide/N-doped graphene oxide nanocomposite for the highly efficient removal of Pb(II) and Cd(II) ions from water. *J. Solid State Chem.* **2019**, *280*, 120963. [CrossRef]
176. Dou, J.; Chen, J.; Huang, Q.; Huang, H.; Mao, L.; Deng, F.; Wen, Y.; Zhu, X.; Zhang, X.; Wei, Y. Preparation of polymer functionalized layered double hydroxide through mussel-inspired chemistry and Kabachnik–Fields reaction for highly efficient adsorption. *J. Environ. Chem. Eng.* **2020**, *8*, 103634. [CrossRef]
177. Wang, J.; Yang, Q.; Zhang, L.; Liu, M.; Hu, N.; Zhang, W.; Zhu, W.; Wang, R.; Suo, Y.; Wang, J. A hybrid monolithic column based on layered double hydroxide-alginate hydrogel for selective solid phase extraction of lead ions in food and water samples. *Food Chem.* **2018**, *257*, 155–162. [CrossRef]
178. Lai, Y.-T.; Huang, Y.-S.; Chen, C.-H.; Lin, Y.-C.; Jeng, H.-T.; Chang, M.-C.; Chen, L.-J.; Lee, C.-Y.; Hsu, P.-C.; Tai, N.-H. Green Treatment of Phosphate from Wastewater Using a Porous Bio-Templated Graphene Oxide/MgMn-Layered Double Hydroxide Composite. *iScience* **2020**, *23*, 101065. [CrossRef] [PubMed]
179. Bing, X.; Zhang, X.; Li, J.; Ng, D.H.L.; Yang, W.; Yang, J. 3D hierarchical tubular micromotors with highly selective recognition and capture for antibiotics. *J. Mater. Chem. A* **2020**, *8*, 2809–2819. [CrossRef]
180. Sanchez, C.; Belleville, P.; Popall, M.; Nicole, L. Applications of advanced hybrid organic–inorganic nanomaterials: From laboratory to market. *Chem. Soc. Rev.* **2011**, *40*, 696–753. [CrossRef] [PubMed]